A comprehensive quantification of global nitrous oxide sources and sinks

Hanqin Tian, Rongting Xu, Josep Canadell, Rona Thompson, Wilfried Winiwarter, Parvadha Suntharalingam, Eric Davidson, Philippe Ciais, Robert Jackson, Greet Janssens-Maenhout, et al.

Article

A comprehensive quantification of global nitrous oxide sources and sinks

https://doi.org/10.1038/s41586-020-2780-0

Received: 28 December 2019

Accepted: 14 August 2020

Published online: 7 October 2020

Check for updates

Hanqin Tian[1]✉, Rongting Xu[1], Josep G. Canadell[2], Rona L. Thompson[3], Wilfried Winiwarter[4,5], Parvadha Suntharalingam[6], Eric A. Davidson[7], Philippe Ciais[8], Robert B. Jackson[9,10,11], Greet Janssens-Maenhout[12,13], Michael J. Prather[14], Pierre Regnier[15], Naiqing Pan[1,16], Shufen Pan[1], Glen P. Peters[17], Hao Shi[1], Francesco N. Tubiello[18], Sönke Zaehle[19], Feng Zhou[20], Almut Arneth[21], Gianna Battaglia[22], Sarah Berthet[23], Laurent Bopp[24], Alexander F. Bouwman[25,26,27], Erik T. Buitenhuis[6,28], Jinfeng Chang[8,29], Martyn P. Chipperfield[30,31], Shree R. S. Dangal[32], Edward Dlugokencky[33], James W. Elkins[33], Bradley D. Eyre[34], Bojie Fu[16,35], Bradley Hall[33], Akihiko Ito[36], Fortunat Joos[22], Paul B. Krummel[37], Angela Landolfi[38,39], Goulven G. Laruelle[15], Ronny Lauerwald[8,15,40], Wei Li[8,41], Sebastian Lienert[22], Taylor Maavara[42], Michael MacLeod[43], Dylan B. Millet[44], Stefan Olin[45], Prabir K. Patra[46,47], Ronald G. Prinn[48], Peter A. Raymond[42], Daniel J. Ruiz[14], Guido R. van der Werf[49], Nicolas Vuichard[8], Junjie Wang[27], Ray F. Weiss[50], Kelley C. Wells[44], Chris Wilson[30,31], Jia Yang[51] & Yuanzhi Yao[1]

Nitrous oxide (N_2O), like carbon dioxide, is a long-lived greenhouse gas that accumulates in the atmosphere. Over the past 150 years, increasing atmospheric N_2O concentrations have contributed to stratospheric ozone depletion[1] and climate change[2], with the current rate of increase estimated at 2 per cent per decade. Existing national inventories do not provide a full picture of N_2O emissions, owing to their omission of natural sources and limitations in methodology for attributing anthropogenic sources. Here we present a global N_2O inventory that incorporates both natural and anthropogenic sources and accounts for the interaction between nitrogen additions and the biochemical processes that control N_2O emissions. We use bottom-up (inventory, statistical extrapolation of flux measurements, process-based land and ocean modelling) and top-down (atmospheric inversion) approaches to provide a comprehensive quantification of global N_2O sources and sinks resulting from 21 natural and human sectors between 1980 and 2016. Global N_2O emissions were 17.0 (minimum–maximum estimates: 12.2–23.5) teragrams of nitrogen per year (bottom-up) and 16.9 (15.9–17.7) teragrams of nitrogen per year (top-down) between 2007 and 2016. Global human-induced emissions, which are dominated by nitrogen additions to croplands, increased by 30% over the past four decades to 7.3 (4.2–11.4) teragrams of nitrogen per year. This increase was mainly responsible for the growth in the atmospheric burden. Our findings point to growing N_2O emissions in emerging economies—particularly Brazil, China and India. Analysis of process-based model estimates reveals an emerging N_2O–climate feedback resulting from interactions between nitrogen additions and climate change. The recent growth in N_2O emissions exceeds some of the highest projected emission scenarios[3,4], underscoring the urgency to mitigate N_2O emissions.

Nitrous oxide (N_2O) is a long-lived stratospheric ozone-depleting substance and greenhouse gas with a current atmospheric lifetime of 116 ± 9 years[1]. The concentration of atmospheric N_2O has increased by more than 20% from 270 parts per billion (ppb) in 1750 to 331 ppb in 2018 (Extended Data Fig. 1), with the fastest growth observed in the past five decades[5,6]. Two key biochemical processes—nitrification and denitrification—control N_2O production in both terrestrial and aquatic ecosystems and are regulated by multiple environmental and biological factors including temperature, water and oxygen levels, acidity, substrate availability[7] (which is linked to nitrogen fertilizer use and livestock manure management) and recycling[8–10]. In the coming decades, N_2O emissions are expected to continue to increase as a result of the growing demand for food, feed, fibre and energy, and an increase in sources from waste generation and industrial processes[4,11,12]. Since 1990, anthropogenic N_2O emissions have been reported annually by Annex I Parties to the United Nations Framework Convention on Climate Change (UNFCCC). More recently, over 190 national signatories to the Paris Agreement have been required to report biannually their

A list of affiliations appears at the end of the paper.

national greenhouse-gas inventory with sufficient detail and transparency to track progress towards their nationally determined contributions. However, these inventories do not provide a full picture of N_2O emissions owing to their omission of natural sources, the limitations in methodology for attributing anthropogenic sources, and missing data for a number of key regions (for example, South America and Africa)[2,9,13]. Moreover, a complete account of all human activities that accelerate the global nitrogen cycle and that interact with the biochemical processes controlling the fluxes of N_2O in both terrestrial and aquatic ecosystems is required[2,8]. Here we present a comprehensive, consistent analysis and synthesis of the global N_2O budget across all sectors, including natural and anthropogenic sources and sinks, using both bottom-up and top-down methods and their cross-constraints. Our assessment enhances understanding of the global nitrogen cycle and will inform policy development for N_2O mitigation, which could help to curb warming to levels consistent with the long-term goal of the Paris Agreement.

A reconciling framework (described in Extended Data Fig. 2) was used to take full advantage of bottom-up and top-down approaches for estimating and constraining sources and sinks of N_2O. Bottom-up approaches include emission inventories, spatial extrapolation of field flux measurements, nutrient budget modelling and process-based modelling for land and ocean fluxes. The top-down approaches combine measurements of N_2O mole fractions with atmospheric transport models in statistical optimization frameworks (inversions) to constrain the sources. Here we constructed a total of 43 flux estimates, including 30 using bottom-up approaches, 5 using top-down approaches, and 8 other estimates using observation and modelling approaches (Methods, Extended Data Fig. 2).

With this extensive data and bottom-up/top-down framework, we established comprehensive global and regional N_2O budgets that include 18 sources and various different chemical sinks. These sources and sinks are further grouped into six categories (Fig. 1, Table 1): (1) natural sources (no anthropogenic effects) including a very small biogenic surface sink; (2) perturbed fluxes from ecosystems induced by changes in climate, carbon dioxide (CO_2) and land cover; (3) direct emissions from nitrogen additions in the agricultural sector (agriculture); (4) other direct anthropogenic sources—including fossil fuel and industry, waste and waste water, and biomass burning; (5) indirect emissions from ecosystems that are either downwind or downstream from the initial release of reactive nitrogen into the environment—including N_2O release after transport and deposition of anthropogenic nitrogen via the atmosphere or water bodies as defined by the Intergovernmental Panel on Climate Change (IPCC)[14]; and (6) the atmospheric chemical sink, for which one value is derived from observations and the other is derived from the inversion models. To quantify and attribute the regional N_2O budget, we further partition the Earth's ice-free land into ten regions (Fig. 2, Supplementary Fig. 1). With the construction of these budgets, we explore the relative temporal and spatial importance of multiple sources and sinks that drive the atmospheric burden of N_2O, their uncertainties, and interactions between anthropogenic forcing and natural fluxes of N_2O as an emerging climate feedback.

The global N_2O budget (2007–2016)

The bottom-up and top-down approaches give consistent estimates of global total N_2O emissions in the decade between 2007 and 2016 to well within their respective uncertainties, with values of 17.0 (minimum–maximum estimates: 12.2–23.5) Tg N yr^{-1} and 16.9 (15.9–17.7) Tg N yr^{-1} for bottom-up and top-down approaches, respectively. The global calculated atmospheric chemical sink (that is, N_2O losses via photolysis and reaction with electronically excited atomic oxygen ($O(^1D)$) in the troposphere and stratosphere) is 13.5 (12.4–14.6) Tg N yr^{-1}. The imbalance of sources and sinks of N_2O derived from the averaged bottom-up and top-down estimates is 4.1 Tg N yr^{-1}. This imbalance agrees well with the observed increase in atmospheric abundance of N_2O between 2007 and 2016 of 3.8–4.8 Tg N yr^{-1} (see Methods). Natural sources from soils and oceans contributed 57% of total emissions (mean: 9.7; min–max: 8.0–12.0 Tg N yr^{-1}) during this time, according to our bottom-up estimate. We further estimate the natural soil flux at 5.6 (4.9–6.5) Tg N yr^{-1} and the ocean flux at 3.4 (2.5–4.3) Tg N yr^{-1} (see Methods).

Anthropogenic sources contributed, on average, 43% to the total N_2O emission (mean: 7.3; min–max: 4.2–11.4 Tg N yr^{-1}), of which direct and indirect emissions from nitrogen additions in agriculture and other sectors contributed around 52% and around 18%, respectively. Of the remaining anthropogenic emissions, about 27% were from other direct anthropogenic sources including fossil fuel and industry (around 13%), with about 3% from perturbed fluxes caused by changes in climate, CO_2 or land cover.

Four decades of the global N_2O budget

The atmospheric N_2O burden increased from 1,462 Tg N in the 1980s to 1,555 Tg N in 2007–2016, with a possible uncertainty of ±20 Tg N. Our results (Table 1) show a substantial increase in global N_2O emissions that is primarily driven by anthropogenic sources, as natural sources remained relatively steady throughout the study period. Global N_2O emissions obtained from our bottom-up and top-down approaches are comparable in magnitude during 1998–2016, but top-down results imply a larger inter-annual variability (1.0 Tg N yr^{-1}; Extended Data Fig. 3a). Bottom-up and top-down approaches diverge when estimating the magnitude of land emissions compared with ocean emissions, although they are consistent with respect to trends. Specifically, the bottom-up land estimate during 1998–2016 was on average 1.8 Tg N yr^{-1} higher than the top-down estimate, but showed a slightly slower rate of increase of 0.8 ± 0.2 Tg N yr^{-1} per decade (95% confidence interval; $P < 0.05$) compared with 1.1 ± 0.6 Tg N yr^{-1} per decade ($P < 0.05$) from the top-down approach (Extended Data Fig. 3b). Since 2005, the difference in the magnitude of emissions between the two approaches has become smaller owing to a large increase in emission—particularly in South America, Africa and East Asia—that is inferred by the top-down approach (Extended Data Fig. 3d, f, i). Oceanic N_2O emissions from the bottom-up approach (3.6 (2.7–4.5) Tg N yr^{-1}) indicate a slight decline at a rate of 0.06 Tg N yr^{-1} per decade ($P < 0.05$), whereas the top-down approach gives a higher but stable value of 5.1 (3.4–7.1) Tg N yr^{-1} during 1998–2016 (Table 1).

On the basis of bottom-up approaches, anthropogenic N_2O emissions increased from 5.6 (3.6–8.7) Tg N yr^{-1} in the 1980s to 7.3 (4.2–11.4) Tg N yr^{-1} in 2007–2016, at a rate of 0.6 ± 0.2 Tg N yr^{-1} per decade ($P < 0.05$). Up to 87% of this increase results from direct emission from agriculture (71%) and indirect emission from anthropogenic nitrogen additions into soils (16%). Direct soil emission from fertilizer application is the major source of increases in emission from agriculture, followed by a small but notable increase in emissions from livestock manure and aquaculture. Model-based estimates of direct soil emissions[15–17] show a faster increase than in the three inventories used in our study (see Methods; Extended Data Fig. 4a); this is largely attributed to the interactive effects between climate change and nitrogen additions, as well as spatio-temporal variability in environmental factors such as rainfall and temperature, that modulate the N_2O yield from nitrification and denitrification. This result is in line with the increased emission factor deduced from the top-down estimates, in which the inversion-based soil emissions increased at a faster rate than suggested by the IPCC Tier 1 emission factor[14] (which assumes a linear response), especially after 2009 (ref. [18]). The remaining causes of the increase are attributed to other direct anthropogenic sources (6%) and perturbed fluxes from changes in climate, CO_2 or land cover (8%). The contribution from fossil fuel and industry emissions decreased rapidly between 1980 and 2000, largely due to the installation of emissions-abatement equipment in industrial facilities that produce nitric and adipic acid. However, after

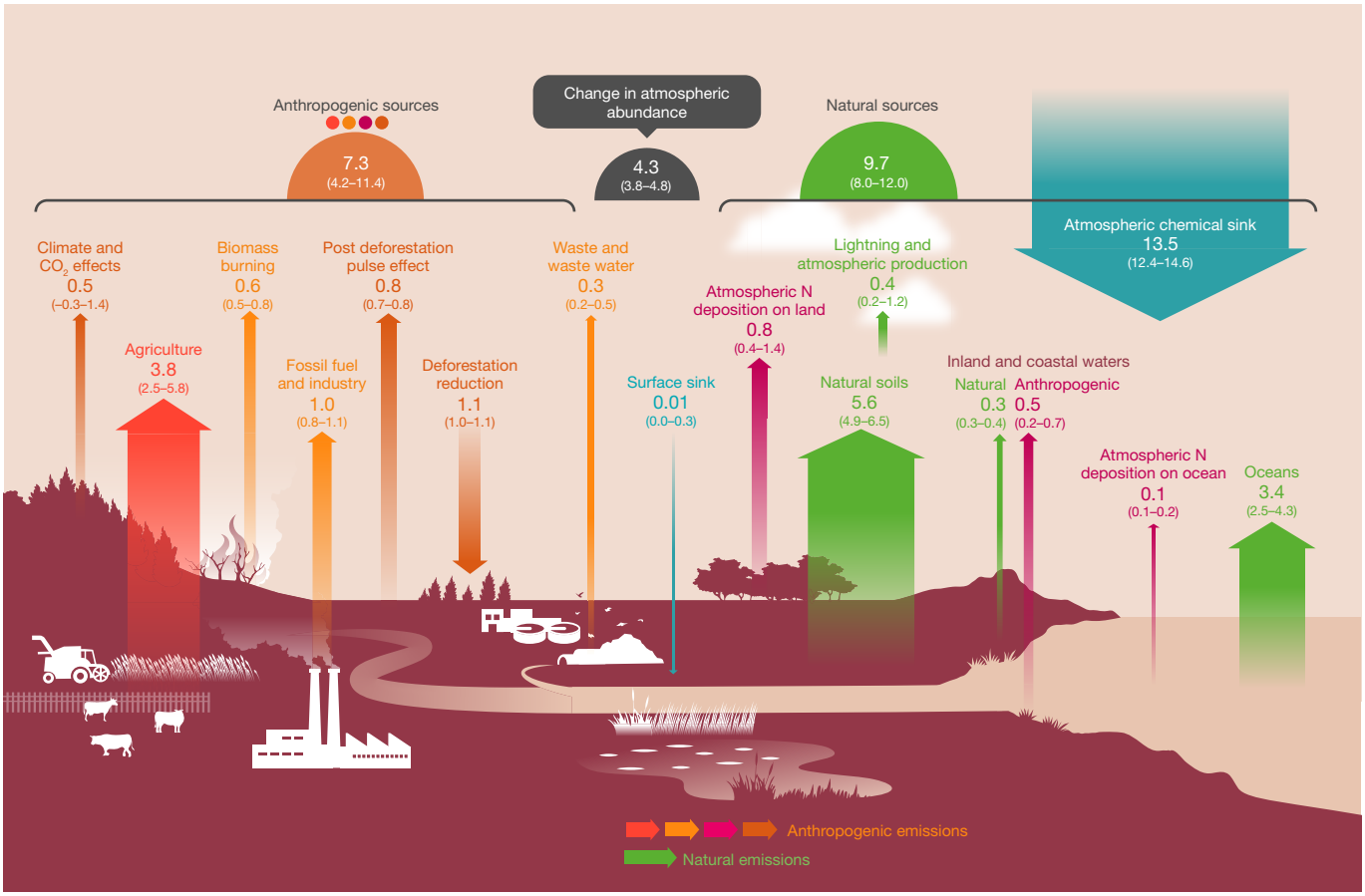

Fig. 1 | Global N_2O budget for 2007–2016. The coloured arrows represent N_2O fluxes (in Tg N yr^{-1} for 2007–2016) as follows: red, direct emissions from nitrogen additions in the agricultural sector (agriculture); orange, emissions from other direct anthropogenic sources; maroon, indirect emissions from anthropogenic nitrogen additions; brown, perturbed fluxes from changes in climate, CO_2 or land cover; green, emissions from natural sources. The anthropogenic and natural N_2O sources are derived from bottom-up estimates. The blue arrows represent the surface sink and the observed atmospheric chemical sink, of which about 1% occurs in the troposphere. The total budget (sources + sinks) does not exactly match the observed atmospheric accumulation, because each of the terms has been derived independently and we do not force top-down agreement by rescaling the terms. This imbalance readily falls within the overall uncertainty in closing the N_2O budget, as reflected in each of the terms. The N_2O sources and sinks are given in Tg N yr^{-1}. Copyright the Global Carbon Project.

2000, such emissions began to increase slowly, owing to increasing fossil fuel combustion (Extended Data Fig. 5a, b).

Our analysis of process-based model estimates indicates that soil N_2O emissions have accelerated substantially as a result of climate change since the early 1980s, and this has offset the reduction due to feedback with increased CO_2 concentration and climate (Extended Data Fig. 6a). Increased CO_2 concentrations enhance plant growth and thus increase nitrogen uptake, which in turn decreases soil N_2O emissions[16,19]. Conversion of land from tropical mature forests, which have higher N_2O emissions, to pastures and other unfertilized agricultural lands has considerably reduced global natural N_2O emissions[11,20,21]. This decrease, however, has been partly offset by an increase in soil N_2O emissions attributed to the temporary increase in emissions after deforestation (the post-deforestation pulse effect) and to background emissions from converted croplands or pastures[21] (see Methods; Extended Data Fig. 7).

From the ensemble of process-based land model emissions[15,16], we estimate a global agricultural soil emission factor of 1.8% (1.3%–2.3%), which is considerably larger than the IPCC Tier 1 default for direct emission of 1%. This higher emission factor, derived from process-based models, suggests a strong interactive effect between nitrogen additions and other global environmental changes (Table 1, 'Perturbed fluxes from climate, atmospheric CO_2 and land cover change'). Previous field experiments reported a better fit to local observations of soil N_2O emissions when assuming a nonlinear response to fertilizer nitrogen inputs under varied climate and soil conditions[17,22]. The nonlinear response is also likely to be associated with long-term nitrogen accumulation in agricultural soils from nitrogen fertilizer use and in aquatic systems from nitrogen loads (the legacy effect)[18,23], which provides more substrate for microbial processes[18,24]. The increasing N_2O emissions estimated by process-based models[16] also suggest that recent climate change—particularly warming—could have boosted soil nitrification and denitrification processes, contributing to the growing trend in N_2O emissions together with increasing nitrogen additions to agricultural soils[16,25–27] (Extended Data Fig. 8).

Regional N_2O budgets (2007–2016)

Bottom-up approaches give estimates of N_2O emissions in each of the five source categories, whereas top-down approaches provide only total emissions (Fig. 2). Bottom-up and top-down approaches indicate that Africa was the largest source of N_2O in the last decade, followed by South America (Fig. 2). Bottom-up and top-down approaches agree well regarding the magnitudes and trends of N_2O emissions from South Asia and Oceania (Extended Data Fig. 3j, l). For the remaining regions, bottom-up and top-down estimates are comparable in terms of trends but diverge when estimating the strengths of the sources. Clearly, much more work on regional N_2O budgets is needed, particularly for South America and Africa where there are larger differences between bottom-up and top-down estimates and larger uncertainties in each

Table 1 | The global N_2O budget in the 1980s, 1990s, 2000s and 2007–2016

		1980s			1990s			2000s			2007–2016		
Anthropogenic sources		**Mean**	**Min.**	**Max.**	**Mean**	**Min.**	**Max.**	**Mean**	**Min.**	**Max.**	**Mean**	**Min.**	**Max.**
Direct emissions from nitrogen additions in the agricultural sector (Agriculture)	Direct soil emissions	1.5	0.9	2.6	1.7	1.1	3.1	2.0	1.3	3.4	2.3	1.4	3.8
	Manure left on pasture	0.9	0.7	1.0	1.0	0.7	1.1	1.1	0.8	1.2	1.2	0.9	1.3
	Manure management	0.3	0.2	0.4	0.3	0.2	0.4	0.3	0.2	0.5	0.3	0.2	0.5
	Aquaculture	0.01	0.00	0.03	0.03	0.01	0.1	0.1	0.02	0.2	0.1	0.02	0.2
	Subtotal	**2.6**	**1.8**	**4.1**	**3.0**	**2.1**	**4.8**	**3.4**	**2.3**	**5.2**	**3.8**	**2.5**	**5.8**
Other direct anthropogenic sources	Fossil fuels and industry	0.9	0.8	1.1	0.9	0.9	1.0	0.9	0.8	1.0	1.0	0.8	1.1
	Waste and waste water	0.2	0.1	0.3	0.3	0.2	0.4	0.3	0.2	0.4	0.3	0.2	0.5
	Biomass burning	0.7	0.7	0.7	0.7	0.6	0.8	0.6	0.6	0.6	0.6	0.5	0.8
	Subtotal	**1.8**	**1.6**	**2.1**	**1.9**	**1.7**	**2.1**	**1.8**	**1.6**	**2.1**	**1.9**	**1.6**	**2.3**
Indirect emissions from anthropogenic nitrogen additions	Inland waters, estuaries, coastal zones	0.4	0.2	0.5	0.4	0.2	0.5	0.4	0.2	0.6	0.5	0.2	0.7
	Atmospheric nitrogen deposition on land	0.6	0.3	1.2	0.7	0.4	1.4	0.7	0.4	1.3	0.8	0.4	1.4
	Atmospheric nitrogen deposition on ocean	0.1	0.1	0.2	0.1	0.1	0.2	0.1	0.1	0.2	0.1	0.1	0.2
	Subtotal	**1.1**	**0.6**	**1.9**	**1.2**	**0.7**	**2.1**	**1.2**	**0.6**	**2.1**	**1.3**	**0.7**	**2.2**
Perturbed fluxes from climate/CO_2/land cover change	CO_2 effect	−0.2	−0.3	0.0	−0.2	−0.4	0.0	−0.3	−0.5	0.1	−0.3	−0.6	0.1
	Climate effect	0.4	0.0	0.8	0.5	0.1	0.9	0.7	0.3	1.2	0.8	0.3	1.3
	Post-deforestation pulse effect	0.7	0.6	0.8	0.7	0.6	0.8	0.7	0.7	0.8	0.8	0.7	0.8
	Long-term effect of reduced mature forest area	−0.8	−0.8	−0.9	−0.9	−0.8	−1.0	−1.0	−0.9	−1.1	−1.1	−1.0	−1.1
	Subtotal	**0.1**	**−0.4**	**0.7**	**0.1**	**−0.5**	**0.7**	**0.2**	**−0.4**	**0.9**	**0.2**	**−0.6**	**1.1**
Anthropogenic total		**5.6**	**3.6**	**8.7**	**6.2**	**3.9**	**9.7**	**6.7**	**4.1**	**10.3**	**7.3**	**4.2**	**11.4**
Natural fluxes													
Natural soils baseline		5.6	4.9	6.6	5.6	4.9	6.5	5.6	5.0	6.5	5.6	4.9	6.5
Ocean baseline		3.6	3.0	4.4	3.5	2.8	4.4	3.5	2.7	4.3	3.4	2.5	4.3
Natural (inland waters, estuaries, coastal zones)		0.3	0.3	0.4	0.3	0.3	0.4	0.3	0.3	0.4	0.3	0.3	0.4
Lightning and atmospheric production		0.4	0.2	1.2	0.4	0.2	1.2	0.4	0.2	1.2	0.4	0.2	1.2
Surface sink		−0.01	0.00	−0.3	−0.01	0.00	−0.3	−0.01	0.00	−0.3	−0.01	0.00	−0.3
Natural total		**9.9**	**8.5**	**12.2**	**9.8**	**8.3**	**12.1**	**9.8**	**8.2**	**12.0**	**9.7**	**8.0**	**12.0**
Bottom-up total source		15.5	12.1	20.9	15.9	12.2	21.7	16.4	12.3	22.4	17.0	12.2	23.5
Top-down ocean								5.1	3.1	7.2	5.1	3.4	7.1
Top-down land								10.8	9.3	12.5	11.8	10.6	13.8
Top-down total source								15.9	15.1	16.9	16.9	15.9	17.7
Top-down stratospheric sink								12.1	11.4	13.1	12.4	11.7	13.3
Observed atmospheric chemical sink[a]								13.3	12.2	14.4	13.5	12.4	14.6
Change in atmospheric abundance[b]								**3.7**	**3.2**	**4.2**	**4.3**	**3.8**	**4.8**
Atmospheric burden		**1,462**	**1,442**	**1,482**	**1,493**	**1,472**	**1,514**	**1,531**	**1,510**	**1,552**	**1,555**	**1,533**	**1,577**

Bottom-up estimates include four categories of anthropogenic source and one category for natural sources and sinks. The sources and sinks of N_2O are given in Tg N yr^{-1}. The atmospheric burden is given in Tg N.

[a]Calculated from satellite observations with a photolysis model (about 1% of this sink occurs in the troposphere).

[b]Calculated from the combined NOAA and AGAGE record of surface N_2O, and adopting the uncertainty of the IPCC Assessment Report 5 (Chapter 6)[2]. Detailed information on calculating each sub-category is shown in Supplementary Tables 1–13.

approach. Advancing the understanding and model representation of key processes responsible for N_2O emissions from land and ocean are priorities to reduce uncertainties in bottom-up estimates. Atmospheric observations in underrepresented regions of the world and better atmospheric transport models are essential to reduce uncertainty in top-down estimates, whereas more accurate activity data and robust emission factors are critical for greenhouse-gas inventories (see Methods for additional discussion on uncertainty).

According to estimates from the Global N_2O Model Intercomparison Project[16], natural soil emissions dominate (to different extents) in tropical and sub-tropical regions. Soil N_2O emissions in the tropics (0.1 ± 0.04 g N m^{-2} yr^{-1}) are about 50% higher than the global average, because many lowland, highly weathered tropical soils have excess nitrogen relative to phosphorus[20]. Total anthropogenic emissions in the 10 terrestrial regions (Fig. 2) were highest in East Asia (1.5 (0.8–2.6) Tg N yr^{-1}), followed by North America, Africa and Europe. High direct

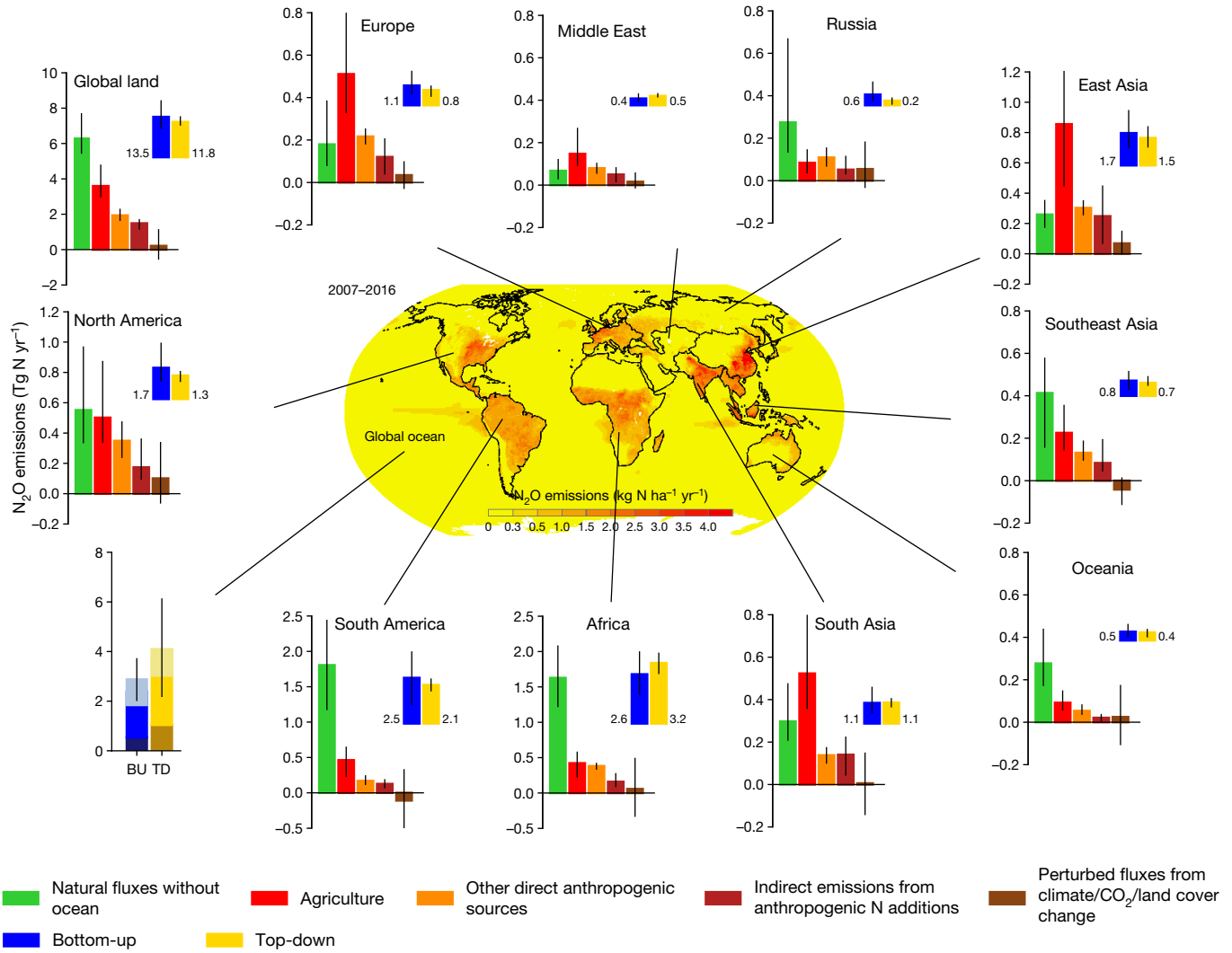

Fig. 2 | Regional N_2O sources in the decade 2007–2016. The Earth's ice-free land is partitioned into ten regions: North America, South America, Europe, Middle East, Africa, Russia, East Asia, South Asia, Southeast Asia and Oceania. Each subplot shows the emissions from five sub-sectors using bottom-up approaches, followed by the sum of these five categories using bottom-up approaches (blue) and the estimates from top-down approaches (yellow). Bottom-up and top-down estimates of ocean emissions are shown at the bottom left (from bottom to top, lighter to darker, the contributions from the 30°–90° N, 30° S–30° N and 90°–30° S regions). Error bars indicate the spread between the minimum and the maximum values. The centre map shows the spatial distribution of 10-year average N_2O emissions from land and ocean based on the land and ocean models. Per capita N_2O emission (kg N per capita per year) during 2007–2016 is shown in Supplementary Fig. 2. The map was created using ESRI ArcMap 10.4.1.

agricultural N_2O emissions can be attributed to the large-scale application of synthetic nitrogen fertilizers in East Asia, Europe, South Asia and North America, which together consume over 80% of the world's synthetic nitrogen fertilizers[28]. By contrast, direct agricultural emissions from Africa and South America mainly arise from livestock manure that is deposited in pastures and rangelands[28,29]. East Asia contributed 71%–79% of global aquaculture N_2O emissions; South Asia and Southeast Asia together contributed 10%–20% (refs. [30,31]). Indirect emissions have a moderate role in the total N_2O budget, with the highest emission in East Asia (0.3 (0.1–0.5) Tg N yr^{-1}). Other direct anthropogenic sources together contribute N_2O emissions of approximately 0.2–0.4 Tg N yr^{-1} in each of East Asia, Africa, North America and Europe.

Both bottom-up and top-down estimates of ocean N_2O emissions for northern, tropical and southern ocean regions (90° N–30° N, 30° N–30° S and 30° S–90° S, respectively) reveal that the tropical oceans contribute over 50% to the global oceanic N_2O source. In particular, the upwelling regions of the equatorial Pacific, Indian and tropical Atlantic (Fig. 3) provide considerable sources of N_2O[32–34]. Bottom-up estimates suggest that the southern ocean region is the second largest contributor, with emissions around twice as high as those from the northern oceans (53% tropical oceans, 31% southern oceans, 17% northern oceans), in line with their respective areas. Top-down estimates, however, suggest approximately equal contributions from the southern and northern ocean regions.

Four decades of anthropogenic N_2O emissions

Trends in anthropogenic emissions were found to vary among regions (Fig. 3). Fluxes from Europe and Russia decreased by a total of 0.6 (0.5–0.7) Tg N yr^{-1} over the 37 years from 1980 to 2016. The decrease in Europe is associated with successful emissions abatement in industry as well as agricultural policies, whereas the decrease in Russia is associated with the collapse of the agricultural cooperative system after 1990. By contrast, fluxes from the remaining eight regions increased by a total of 2.9 (2.4–3.4) Tg N yr^{-1} (Fig. 3), of which 34% came from East Asia, 18% from Africa, 18% from South Asia, 13% from South America and 6% from North America, with the remaining increase attributed to the three other regions.

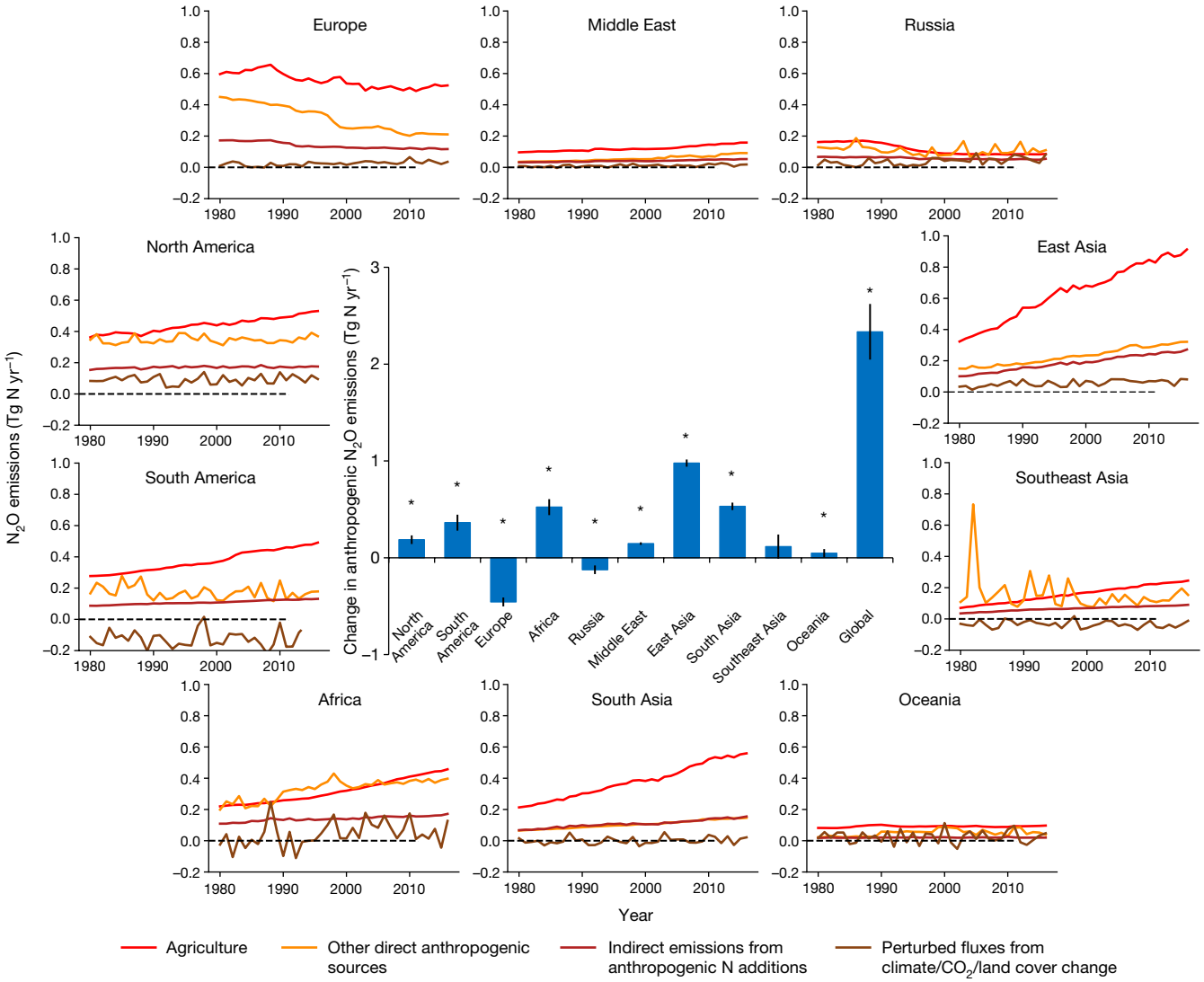

Fig. 3 | Ensembles of regional anthropogenic N_2O emissions over the period 1980–2016. The bar chart in the centre shows the accumulated changes in regional and global N_2O emissions during the study period of 1980–2016. Error bars indicate the 95% confidence interval for the average of accumulated changes. The Mann–Kendall test was performed to examine a monotonic increasing or decreasing trend in the estimated ensemble N_2O emissions globally and for each region over the period 1980–2016. The accumulated changes were calculated from the linear regressed annual change rate (Tg N yr^{-2}) multiplied by 37 years. All regions except Southeast Asia show a significant increasing or decreasing trend in the estimated ensemble N_2O emissions during the study period. *$P < 0.05$.

The relative importance of each anthropogenic source to the total increase in emission differs among regions. East Asia, South Asia, Africa and South America show larger increases in total agricultural N_2O emissions (direct and indirect) compared with the remaining six regions during 1980–2016 (Fig. 3). Southeast Asia, North America and the Middle East also show increasing direct N_2O emissions, but to a smaller extent. Increasing indirect emissions in East Asia, South Asia, Africa and South America on average constitute 20% of total agricultural N_2O emissions and largely result from the considerable increase in fertilizer nitrogen inputs to agricultural soils[35,36]. The fastest increase in emissions from other direct anthropogenic sources was found in East Asia, and is primarily due to rapidly increasing industrial emissions. Africa and South Asia also show a rapid increase in emissions, arising from fossil fuels and industry, and from waste and waste water.

Our findings point to growing N_2O emissions in emerging economies—particularly Brazil, China and India. For example, we find here that the substantial increases in livestock manure left on pasture and in fertilizer use caused an increase of approximately 120% in Brazilian agricultural N_2O emissions during 1980–2016 (Extended Data Fig. 9). In addition to fertilizer applications, the production of global livestock manure has been growing steadily, in line with increased livestock numbers[15,28]. Growing demand for meat and dairy products has substantially increased global N_2O emissions from livestock manure production and management associated with the expansion of pastures and grazing land[37]. Meanwhile, expansion of feed crop production to support the growth of livestock could further enhance global N_2O emissions[37,38]. Likewise, increasing demand for fish has resulted in a fivefold increase in global N_2O production from aquaculture since the late 1980s[39], and demand is projected to increase further[40]; however, this remains a small fraction (less than 1%) of total N_2O emissions.

The acceleration of global N_2O emissions resulting from anthropogenic sources is apparent from both bottom-up and top-down estimates. It currently tracks the highest Representative Concentration Pathway[4] (RCP) in the fifth assessment report of the IPCC[2], RCP 8.5, and exceeds all the Shared Socioeconomic Pathways (SSPs)[3] in the Coupled Model Intercomparison Project Phase 6 (CMIP6) for the sixth

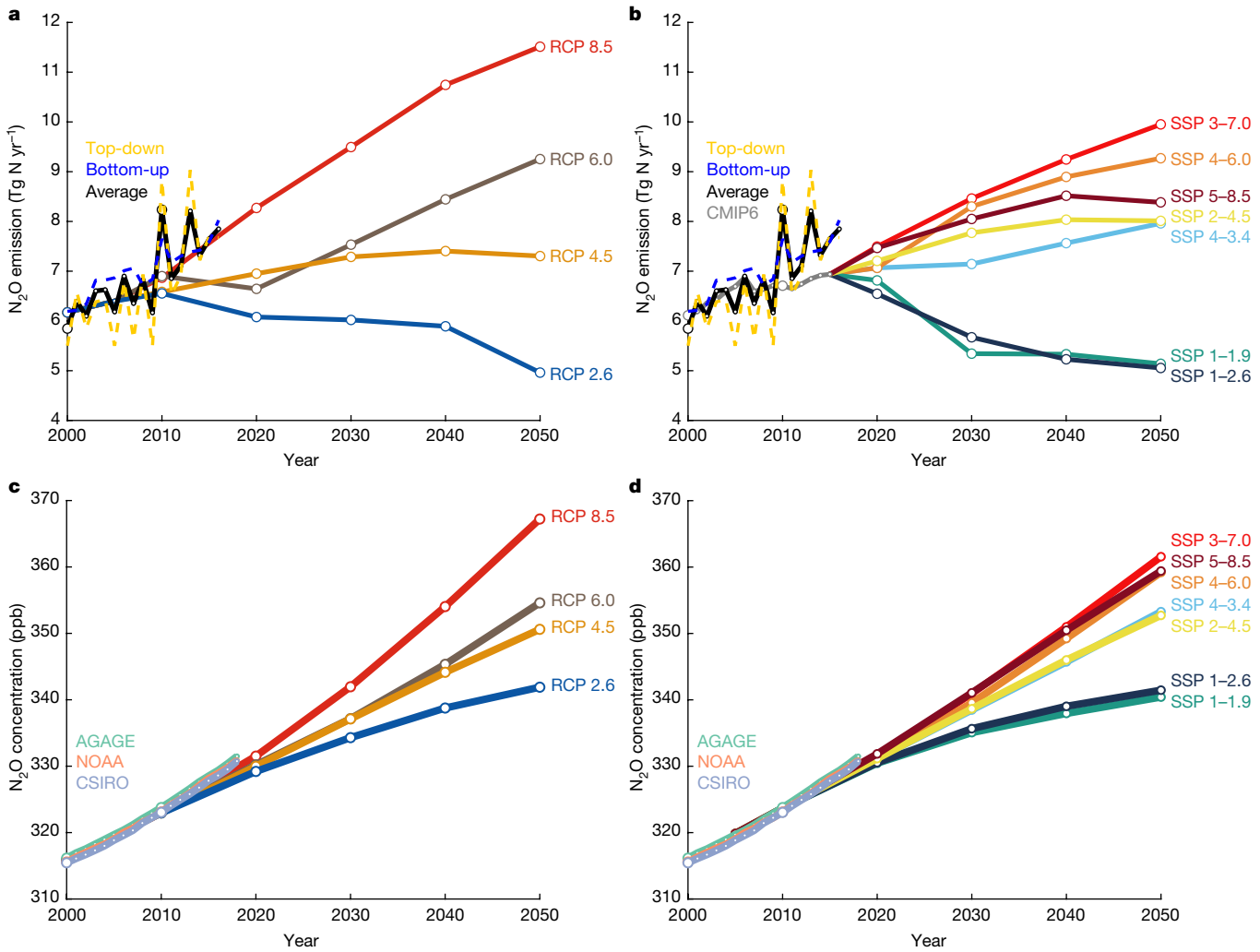

Fig. 4 | Historical and projected global anthropogenic N_2O emissions and concentrations. a–**d**, Global anthropogenic N_2O emissions (**a**, **b**) and concentrations (**c**, **d**) compared to the four RCPs in the IPCC assessment report 5 (**a**, **c**; ref. [2]) and the new marker scenarios based on the SSPs used in CMIP6 (**b**, **d**; ref. [48]). The historical emissions data are represented as the mean of the bottom-up and top-down estimates of anthropogenic N_2O emissions, whereas the historical atmospheric concentration data are from the three available observation networks: AGAGE, NOAA, and CSIRO. Top-down anthropogenic emissions were calculated by subtracting natural fluxes derived from bottom-up approaches. To aid the comparison, the four RCPs were shifted down so that the 2005 value is equal to the 2000–2009 average of the mean of top-down and bottom-up estimates. The SSPs are harmonized[3] to match the historical emissions used in CMIP6[49]; Extended Data Fig. 10 shows the unharmonized data.

assessment report of the IPCC (Fig. 4). Observed atmospheric N_2O concentrations are beginning to exceed predicted levels across all scenarios. Emissions need to be reduced to a level that is consistent with or below that of RCP 2.6 or SSP 1–2.6 in order to limit warming to well below the 2 °C target of the Paris Agreement. Failure to include N_2O within climate mitigation strategies will necessitate even greater abatement of CO_2 and methane. Although N_2O mitigation is difficult because nitrogen is the key limiting nutrient in agricultural production, this study demonstrates that effective mitigation actions have reduced emissions in some regions—such as Europe—through technological improvements in industry and improved efficiency of nitrogen use in agriculture.

There are numerous mitigation options in the agriculture sector that are available for immediate deployment, including increasing the efficiency of nitrogen use both in animal production (through the tuning of feed rations to reduce nitrogen excretion) and in crop production (through precision delivery of nitrogen fertilizers, split applications and better timing to match nitrogen applications to crop demand, conservation tillage, prevention of waterlogging, and the use of nitrification inhibitors[41,42]). Success stories include the stabilization or reduction of N_2O emissions through improving nitrogen use efficiency in the United States and Europe, while maintaining or even increasing crop yields[42,43]. There is every reason to expect that additional implementation of more sustainable practices and emerging technologies will lead to further reduction of emissions in these regions. For example, N_2O emissions from European agricultural soils decreased by 21% between 1990 and 2010—a decline attributed to the implementation of the Nitrates Directive (an agricultural policy that favours optimization and reduction of fertilizer use as well as water protection legislation)[44]. For regions in which emissions are growing, an immediate opportunity lies in the reduction of excess fertilizer use along with the implementation of more sustainable agricultural practices; together, these strategies have been shown to increase crop yields, reduce N_2O emissions, increase water quality and increase farm income[45]. In addition, N_2O emissions can be efficiently abated in the chemical industry[11,41,46,47]. This has been achieved successfully in nitric

acid plants in the European Union, where industrial N_2O emissions decreased from 11% to 3% of total emissions between 2007 and 2012 (ref. [44]). Additional strategies available to reduce N_2O emissions include promoting lower meat consumption in some parts of the world[9] and reducing food waste[11].

We present the most comprehensive, to our knowledge, global N_2O budget so far, with a detailed sectorial and regional attribution of sources and sinks. Each of the past four decades has had higher global N_2O emissions than the last, and overall, agricultural activities have dominated the growth in emissions. Total industrial emissions have been quite stable, with increased emissions from the fossil fuel sector offset to some extent by the decline in emissions in other industrial sectors as a result of successful abatement policies. We also highlight a number of complex interactions between N_2O fluxes and human-driven changes, the effect of which on the global atmospheric N_2O growth rate was previously unknown. These interactions include the effects of climate change, increasing atmospheric CO_2 and deforestation. Cumulatively, these exert a relatively small effect on the overall increase in N_2O concentrations; however, individual flux components—such as the increasing positive climate–N_2O feedback—are considerable. These fluxes are not currently included when reporting national greenhouse gas emissions. We further find that Brazil, China and India dominate the regional contributions to the increase in global N_2O emissions over the most recent decade. Our extensive database and modelling capability fill current gaps in national and regional emissions inventories. Future research is needed to further constrain complex biogeochemical interactions between natural and anthropogenic fluxes and global environmental changes, which could lead to considerable feedback in the future. Reducing excess nitrogen applications to croplands and adopting precision fertilizer application methods provide the greatest immediate opportunities for the abatement of N_2O emissions.

Online content

Any methods, additional references, Nature Research reporting summaries, source data, extended data, supplementary information, acknowledgements, peer review information; details of author contributions and competing interests; and statements of data and code availability are available at https://doi.org/10.1038/s41586-020-2780-0.

1. Prather, M. J. et al. Measuring and modeling the lifetime of nitrous oxide including its variability. *J. Geophys. Res. D* **120**, 5693–5705 (2015).
2. Ciais, P. et al. in *Climate Change 2013: The Physical Science* Basis (eds Stocker, T. F. et al.) Ch. 6 (IPCC, Cambridge Univ. Press, 2013).
3. Gidden, M. J. et al. Global emissions pathways under different socioeconomic scenarios for use in CMIP6: a dataset of harmonized emissions trajectories through the end of the century. *Geosci. Model Dev.* **12**, 1443–1475 (2019).
4. Davidson, E. A. Representative concentration pathways and mitigation scenarios for nitrous oxide. *Environ. Res. Lett.* **7**, 024005 (2012).
5. Hall, B., Dutton, G. & Elkins, J. The NOAA nitrous oxide standard scale for atmospheric observations. *J. Geophys. Res. D* **112**, D09305 (2007).
6. Prinn, R. G. et al. History of chemically and radiatively important atmospheric gases from the Advanced Global Atmospheric Gases Experiment (AGAGE). *Earth Syst. Sci. Data* **10**, 985–1018 (2018).
7. Butterbach-Bahl, K., Baggs, E. M., Dannenmann, M., Kiese, R. & Zechmeister-Boltenstern, S. Nitrous oxide emissions from soils: how well do we understand the processes and their controls? *Phil. Trans. R. Soc. Lond. B* **368**, 20130122 (2013).
8. Tian, H. et al. The terrestrial biosphere as a net source of greenhouse gases to the atmosphere. *Nature* **531**, 225–228 (2016).
9. United Nations Environment Programme & Suntharalingam, P. *Drawing Down N_2O to Protect Climate and the Ozone Layer* (United Nations Environment Programme, 2013).
10. Park, S. et al. Trends and seasonal cycles in the isotopic composition of nitrous oxide since 1940. *Nat. Geosci.* **5**, 261–265 (2012).
11. Davidson, E. A. & Kanter, D. Inventories and scenarios of nitrous oxide emissions. *Environ. Res. Lett.* **9**, 105012 (2014).
12. Reay, D. S. et al. Global agriculture and nitrous oxide emissions. *Nat. Clim. Change* **2**, 410–416 (2012).
13. Syakila, A. & Kroeze, C. The global nitrous oxide budget revisited. *Greenhouse Gas Meas. Manage.* **1**, 17–26 (2011).
14. IPCC 2006. *2006 IPCC Guidelines for National Greenhouse Gas Inventories* (eds Eggleston, H. S. et al.) (IGES, 2006).
15. Dangal, S. R. et al. Global nitrous oxide emissions from pasturelands and rangelands: magnitude, spatio-temporal patterns and attribution. *Glob. Biogeochem. Cycles* **33**, 200–222 (2019).
16. Tian, H. et al. Global soil nitrous oxide emissions since the preindustrial era estimated by an ensemble of terrestrial biosphere models: magnitude, attribution, and uncertainty. *Glob. Change Biol.* **25**, 640–659 (2019).
17. Wang, Q. et al. Data-driven estimates of global nitrous oxide emissions from croplands. *Natl Sci. Rev.* **7**, 441–452 (2020).
18. Thompson, R. L. et al. Acceleration of global N_2O emissions seen from two decades of atmospheric inversion. *Nat. Clim. Change* **9**, 993–998 (2019).
19. Zaehle, S., Ciais, P., Friend, A. D. & Prieur, V. Carbon benefits of anthropogenic reactive nitrogen offset by nitrous oxide emissions. *Nat. Geosci.* **4**, 601–605 (2011).
20. Davidson, E. A. et al. Recuperation of nitrogen cycling in Amazonian forests following agricultural abandonment. *Nature* **447**, 995–998 (2007).
21. Verchot, L. V. et al. Land use change and biogeochemical controls of nitrogen oxide emissions from soils in eastern Amazonia. *Glob. Biogeochem. Cycles* **13**, 31–46 (1999).
22. Shcherbak, I., Millar, N. & Robertson, G. P. Global metaanalysis of the nonlinear response of soil nitrous oxide (N_2O) emissions to fertilizer nitrogen. *Proc. Natl Acad. Sci. USA* **111**, 9199–9204 (2014).
23. Van Meter, K. J., Basu, N. B., Veenstra, J. J. & Burras, C. L. The nitrogen legacy: emerging evidence of nitrogen accumulation in anthropogenic landscapes. *Environ. Res. Lett.* **11**, 035014 (2016).
24. Firestone, M. K. & Davidson, E. A. Microbiological basis of NO and N_2O production and consumption in soil. In *Exchange of Trace Gases Between Terrestrial Ecosystems and the Atmosphere* Vol. 47 (Andreae, M. O. & Schimel, D. S.) 7–21 (Wiley, 1989).
25. Griffis, T. J. et al. Nitrous oxide emissions are enhanced in a warmer and wetter world. *Proc. Natl Acad. Sci. USA* **114**, 12081–12085 (2017).
26. Pärn, J. et al. Nitrogen-rich organic soils under warm well-drained conditions are global nitrous oxide emission hotspots. *Nat. Commun.* **9**, 1135 (2018).
27. Smith, K. The potential for feedback effects induced by global warming on emissions of nitrous oxide by soils. *Glob. Change Biol.* **3**, 327–338 (1997).
28. *The Food and Agriculture Organization of the United Nations Statistics* (FAO, accessed 7 July 2019); https://www.fao.org/faostat/en/#data/.
29. Xu, R. et al. Increased nitrogen enrichment and shifted patterns in the world's grassland: 1860–2016. *Earth Syst. Sci. Data* **11**, 175–187 (2019).
30. Beusen, A. H., Bouwman, A. F., Van Beek, L. P., Mogollón, J. M. & Middelburg, J. J. Global riverine N and P transport to ocean increased during the 20th century despite increased retention along the aquatic continuum. *Biogeosciences* **13**, 2441–2451 (2016).
31. MacLeod, M., Hasan, M. R., Robb, D. H. F. & Mamun-Ur-Rashid, M. *Quantifying and Mitigating Greenhouse Gas Emissions from Global Aquaculture* FAO Fisheries and Aquaculture technical paper no. 626 (FAO, 2019).
32. Buitenhuis, E. T., Suntharalingam, P. & Le Quéré, C. Constraints on global oceanic emissions of N_2O from observations and models. *Biogeosciences* **15**, 2161–2175 (2018).
33. Manizza, M., Keeling, R. F. & Nevison, C. D. On the processes controlling the seasonal cycles of the air–sea fluxes of O_2 and N_2O: a modelling study. *Tellus B* **64**, 18429 (2012).
34. Martinez-Rey, J., Bopp, L., Gehlen, M., Tagliabue, A. & Gruber, N. Projections of oceanic N_2O emissions in the 21st century using the IPSL Earth system model. *Biogeosciences* **12**, 4133–4148 (2015).
35. Maavara, T. et al. Nitrous oxide emissions from inland waters: are IPCC estimates too high? *Glob. Change Biol.* **25**, 473–488 (2019).
36. Yao, Y. et al. Increased global nitrous oxide emissions from streams and rivers in the Anthropocene. *Nat. Clim. Change* **10**, 138–142 (2020).
37. Gerber, P. J. et al. *Tackling Climate Change Through Livestock: A Global Assessment of Emissions and Mitigation Opportunities*. (FAO, 2013).
38. Herrero, M. et al. Biomass use, production, feed efficiencies, and greenhouse gas emissions from global livestock systems. *Proc. Natl Acad. Sci. USA* **110**, 20888–20893 (2013).
39. Yuan, J. et al. Rapid growth in greenhouse gas emissions from the adoption of industrial-scale aquaculture. *Nat. Clim. Change* **9**, 318–322 (2019).
40. Froehlich, H. E., Runge, C. A., Gentry, R. R., Gaines, S. D. & Halpern, B. S. Comparative terrestrial feed and land use of an aquaculture-dominant world. *Proc. Natl Acad. Sci. USA* **115**, 5295–5300 (2018).
41. Winiwarter, W., Höglund-Isaksson, L., Klimont, Z., Schöpp, W. & Amann, M. Technical opportunities to reduce global anthropogenic emissions of nitrous oxide. *Environ. Res. Lett.* **13**, 014011 (2018).
42. Zhang, X. et al. Managing nitrogen for sustainable development. *Nature* **528**, 51–59 (2015).
43. Mueller, N. D. et al. Declining spatial efficiency of global cropland nitrogen allocation. *Glob. Biogeochem. Cycles* **31**, 245–257 (2017).
44. European Environment Agency. *Annual European Union Greenhouse Gas Inventory 1990–2017 and Inventory Report 2019* EEA/PUBL/2019/051 (EEA, 2019).
45. Cui, Z. et al. Pursuing sustainable productivity with millions of smallholder farmers. *Nature* **555**, 363–366 (2018).
46. Kanter, D. et al. A post-Kyoto partner: considering the stratospheric ozone regime as a tool to manage nitrous oxide. *Proc. Natl Acad. Sci. USA* **110**, 4451–4457 (2013).
47. Schneider, L., Lazarus, M. & Kollmuss, A. *Industrial N_2O Projects Under the CDM: Adipic Acid – A Case of Carbon Leakage* SEI working paper WP-US-1006 (Stockholm Environment Institute, 2010).
48. O'Neill, B. C. et al. The Scenario Model Intercomparison Project (ScenarioMIP) for CMIP6. *Geosci. Model Dev.* **9**, 3461–3482 (2016).
49. Gütschow, J. et al. The PRIMAP-hist national historical emissions time series. *Earth Syst. Sci. Data* **8**, 571–603 (2016).

[1]International Center for Climate and Global Change Research, School of Forestry and Wildlife Sciences, Auburn University, Auburn, AL, USA. [2]Global Carbon Project, CSIRO Oceans and Atmosphere, Canberra, Australian Capital Territory, Australia. [3]Norsk Institutt for Luftforskning, NILU, Kjeller, Norway. [4]International Institute for Applied Systems Analysis, Laxenburg, Austria. [5]Institute of Environmental Engineering, University of Zielona Góra, Zielona Góra, Poland. [6]School of Environmental Sciences, University of East Anglia, Norwich, UK. [7]Appalachian Laboratory, University of Maryland Center for Environmental Science, Frostburg, MD, USA. [8]Laboratoire des Sciences du Climat et de l'Environnement, LSCE, CEA CNRS, UVSQ UPSACLAY, Gif sur Yvette, France. [9]Department of Earth System Science, Stanford University, Stanford, CA, USA. [10]Woods Institute for the Environment, Stanford University, Stanford, CA, USA. [11]Precourt Institute for Energy, Stanford University, Stanford, CA, USA. [12]European Commission, Joint Research Centre (JRC), Ispra, Italy. [13]Ghent University, Faculty of Engineering and Architecture, Ghent, Belgium. [14]Department of Earth System Science, University of California Irvine, Irvine, CA, USA. [15]Department of Geoscience, Environment & Society, Université Libre de Bruxelles, Brussels, Belgium. [16]State Key Laboratory of Urban and Regional Ecology, Research Center for Eco-Environmental Sciences, Chinese Academy of Sciences, Beijing, China. [17]CICERO Center for International Climate Research, Oslo, Norway. [18]Statistics Division, Food and Agriculture Organization of the United Nations, Rome, Italy. [19]Max Planck Institute for Biogeochemistry, Jena, Germany. [20]Sino-France Institute of Earth Systems Science, Laboratory for Earth Surface Processes, College of Urban and Environmental Sciences, Peking University, Beijing, China. [21]Karlsruhe Institute of Technology, Institute of Meteorology and Climate Research/Atmospheric Environmental Research, Garmisch-Partenkirchen, Germany. [22]Climate and Environmental Physics, Physics Institute and Oeschger Centre for Climate Change Research, University of Bern, Bern, Switzerland. [23]Centre National de Recherches Météorologiques (CNRM), Université de Toulouse, Météo-France, CNRS, Toulouse, France. [24]LMD-IPSL, Ecole Normale Supérieure / PSL Université, CNRS, Ecole Polytechnique, Sorbonne Université, Paris, France. [25]PBL Netherlands Environmental Assessment Agency, The Hague, The Netherlands. [26]Department of Earth Sciences – Geochemistry, Faculty of Geosciences, Utrecht University, Utrecht, The Netherlands. [27]Key Laboratory of Marine Chemistry Theory and Technology, Ministry of Education, Ocean University of China, Qingdao, China. [28]Tyndall Centre for Climate Change Research, School of Environmental Sciences, University of East Anglia, Norwich, UK. [29]College of Environmental and Resource Sciences, Zhejiang University, Hangzhou, China. [30]National Centre for Earth Observation, University of Leeds, Leeds, UK. [31]Institute for Climate and Atmospheric Science, School of Earth and Environment, University of Leeds, Leeds, UK. [32]Woods Hole Research Center, Falmouth, MA, USA. [33]NOAA Global Monitoring Laboratory, Boulder, CO, USA. [34]Centre for Coastal Biogeochemistry, School of Environment Science and Engineering, Southern Cross University, Lismore, New South Wales, Australia. [35]Faculty of Geographical Science, Beijing Normal University, Beijing, China. [36]Center for Global Environmental Research, National Institute for Environmental Studies, Tsukuba, Japan. [37]Climate Science Centre, CSIRO Oceans and Atmosphere, Aspendale, Victoria, Australia. [38]GEOMAR Helmholtz Centre for Ocean Research Kiel, Kiel, Germany. [39]Istituto di Scienze Marine, Consiglio Nazionale delle Ricerche (CNR), Rome, Italy. [40]Université Paris-Saclay, INRAE, AgroParisTech, UMR ECOSYS, Thiverval-Grignon, France. [41]Ministry of Education Key Laboratory for Earth System Modeling, Department of Earth System Science, Tsinghua University, Beijing, China. [42]Yale School of Forestry and Environmental Studies, New Haven, CT, USA. [43]Land Economy, Environment & Society, Scotland's Rural College (SRUC), Edinburgh, UK. [44]Department of Soil, Water, and Climate, University of Minnesota, St Paul, MN, USA. [45]Department of Physical Geography and Ecosystem Science, Lund University, Lund, Sweden. [46]Research Institute for Global Change, JAMSTEC, Yokohama, Japan. [47]Center for Environmental Remote Sensing, Chiba University, Chiba, Japan. [48]Center for Global Change Science, Massachusetts Institute of Technology, Cambridge, MA, USA. [49]Faculty of Science, Vrije Universiteit, Amsterdam, The Netherlands. [50]Scripps Institution of Oceanography, University of California San Diego, La Jolla, CA, USA. [51]Department of Forestry, Mississippi State University, Mississippi State, MS, USA. [52]e-mail: tianhan@auburn.edu

Methods

Terminology

This study provides an estimation of the global N_2O budget considering all possible sources and all global change processes that can perturb the budget. A total of 18 sources and three sinks of N_2O are identified and grouped into six categories (Fig. 1, Table 1): (1) natural fluxes in the absence of climate change and anthropogenic disturbances including soil emissions, surface sink, ocean emissions, lightning and atmospheric production, and natural emission from inland waters, estuaries, coastal zones (inland and coastal waters); (2) perturbed fluxes from climate/CO_2/land cover change including the effect of CO_2, the effect of climate, the post-deforestation pulse effect, and the long-term effect of reduced mature forest area; (3) direct emissions from nitrogen additions in the agricultural sector ('agriculture') including emissions from direct application of synthetic nitrogen fertilizers and manure (henceforth 'direct soil emissions'), manure left on pasture, manure management and aquaculture; (4) indirect emissions from anthropogenic nitrogen additions including atmospheric nitrogen deposition (NDEP) on land, atmospheric NDEP on ocean, and effects of anthropogenic loads of reactive nitrogen in inland waters, estuaries and coastal zones; (5) other direct anthropogenic sources including fossil fuel and industry, waste and waste water, and biomass burning; and (6) two estimates of stratospheric sinks obtained from atmospheric chemistry transport models and observations, and one tropospheric sink (Table 1, Extended Data Fig. 2).

For the purpose of compiling national greenhouse-gas inventories for reporting data for each country to the climate convention, our anthropogenic N_2O emission categories are aligned with those used in UNFCCC reporting and IPCC 2006 methodologies (Supplementary Table 14). We also provide a detailed comparison of our methodology and quantification with that of the IPCC assessment report 5 (see Supplementary Information section 4, Supplementary Table 15).

Data synthesis

We consider global N_2O emission from land and ocean consisting of natural fluxes and anthropogenic emissions estimated from bottom-up and top-down approaches; however, the top-down approach cannot separate natural and anthropogenic sources.

'Natural soil baseline' emissions were obtained from six terrestrial biosphere models (Global N_2O Model Intercomparison Project (NMIP)[16], Supplementary Tables 16, 17) and reflect a situation without consideration of land use change (for example, deforestation) and without consideration of indirect anthropogenic effects via global change (that is, climate, increased CO_2 and atmospheric nitrogen deposition). Bottom-up oceanic N_2O emissions were based on an inter-comparison of five global ocean biogeochemistry models (Supplementary Table 18). The natural emission from 'Inland water, estuaries, coastal zones' includes coastal upwelling[50] and inland and coastal waters that were obtained from ref. [36], ref. [35] and ref. [51]. Because the data (rivers, reservoirs, and estuaries) provided in ref. [35] and ref. [51] are for the year 2000, we assume that these values are constant during 1980–2016. Ref. [36] provided annual riverine N_2O emissions using the DLEM model during the same period. Here, we averaged estimates from ref. [36] with those from ref. [35]. In addition, we estimated N_2O emissions from global and regional reservoirs in the 2000s, and averaged their estimates with those from ref. [35] to represent emissions from reservoirs during 1980–2016. The estimate for global and regional estuaries and lakes is still based on the long-term averaged values provided by ref. [35] and ref. [51], respectively. We considered the riverine emissions in the year 1900 as equivalent to the natural emission for the DLEM estimate assuming that the nitrogen load from land was negligible in that period[52]. We quantified the contribution of natural sources to total emission from reservoirs, lakes and estuaries at 44% (36%–52%), with consideration of all nitrogen inputs (that is, inorganic, organic, dissolved and particulate forms). We combined the estimate from lightning with that from atmospheric production into an integrated category denoted 'Lightning and atmospheric production'. We make a simplification by considering the category 'Lightning and atmospheric production' as purely natural; however, atmospheric production is affected to some extent by anthropogenic activities through enhancing the concentrations of the reactive species NH_2 and NO_2. This category is in any case very small and the anthropogenic enhancement effect is uncertain. Lightning produces NO_x, the median estimate of which is 5 Tg N yr^{-1} (ref. [53]). We assumed an emission factor of 1% (ref. [54]) and a global estimate of 0.05 (0.02–0.09) Tg N yr^{-1} from lightning. Atmospheric production of N_2O results from the reaction of NH_2 with NO_2 (refs. [55,56]), N with NO_2, and from the oxidation of N_2 by $O(^1D)$[57], all of which constitute an estimated source of 0.3 (0.2–1.1) Tg N yr^{-1}. The estimate of the 'Surface sink' was obtained from ref. [58] and ref. [59].

The anthropogenic sources include four sub-sectors:

(a) Agriculture. This consists of four components: 'Direct soil emissions', 'Manure left on pasture', 'Manure management' and 'Aquaculture'. Data for 'Direct soil emissions' were obtained as the ensemble mean of N_2O emissions from an average of three inventories (EDGAR v4.3.2, FAOSTAT and GAINS), the SRNM/DLEM models and the NMIP/DLEM models. The statistical model SRNM covers only cropland N_2O emissions, the same as the NMIP. Thus, we add the DLEM-based estimate of pasture N_2O emissions into the two estimates in cropland to represent direct agricultural soil emissions (that is, SRNM/DLEM or NMIP/DLEM). The 'Manure left on pasture' and 'Manure management' emissions are the ensemble mean of the values from the EDGAR v4.3.2, FAOSTAT and GAINS databases. Global nitrogen flows (that is, fish feed intake, fish harvest and waste) in freshwater and marine aquaculture were obtained from ref. [30] and refs. [60,61] based on a nutrient budget model for the period 1980–2016. We then calculated global aquaculture N_2O emissions through considering 1.8% loss of nitrogen waste in aquaculture, the same emission factor used in ref. [62] and ref. [31]. The uncertainty range of the emission factor is from 0.5% (ref.[14]) to 5% (ref. [63]), the same range used in the UNEP report[9]. The 'Aquaculture' emission for the period 2007–2016 was estimated through synthesizing multiple sources of data from ref. [62] in 2009, the FAO report[31] in 2013 and our calculations. The estimate of aquaculture N_2O emission before 2009 was from our calculations only.

The estimated direct emissions from agriculture have increased from 2.6 (1.8–4.1) Tg N yr^{-1} in the 1980s to 3.8 (2.5–5.8) Tg N yr^{-1} over the recent decade (2007–2016, Table 1). Specifically, direct soil emission from the application of fertilizers is the major source and increased at a rate of 0.27 ± 0.01 Tg N yr^{-1} per decade ($P < 0.05$; Table 1). Compared with the three global inventories (FAOSTAT, EDGAR v4.3.2, and GAINS), the estimates from process-based models (NMIP/DLEM[15,16]) and a statistical model (SRNM)/DLEM[15,17] exhibited a faster increase (Extended Data Fig. 4a). Over the past four decades, we also found a small but significant increase in emissions from livestock manure (that is, manure left on pasture and manure management) at a rate of 0.1 ± 0.01 Tg N yr^{-1} per decade ($P < 0.05$; Extended Data Fig. 4b-c). Meanwhile, global aquaculture N_2O emissions increased tenfold, however, this flux remains the smallest term in the global budget (Extended Data Fig. 4d).

(b) Other direct anthropogenic sources. This includes 'Fossil fuel and industry', 'Waste and waste water', and 'Biomass burning'. Both 'Fossil fuel and industry' and 'Waste and waste water' are the ensemble means of the values from EDGAR v4.3.2 and GAINS databases. The 'Biomass burning' emission is the ensemble mean of values from FAOSTAT, DLEM and GFED4s databases.

Emissions from a combination of fossil fuel and industry, waste and waste water, and biomass burning increased from 1.8 (1.6–2.1) Tg N yr^{-1} in the 1980s to 1.9 (1.6–2.3) Tg N yr^{-1} over the period 2007–2016 (Table 1). The waste and waste water emission showed a continuous increase at a rate of 0.04 ± 0.01 Tg N yr^{-1} per decade ($P < 0.05$) (Extended Data Fig. 5c). Emissions from biomass burning, estimated on the basis of three data

sources (DLEM, GFED4s, and FAOSTAT), slightly decreased at a rate of −0.03 ± 0.04 Tg N yr^{-1} per decade (P = 0.3) since the 1980s (Extended Data Fig. 5d). This contribution is largely affected by climate and land use change[64,65]. Of the three data sources, the DLEM estimate exhibited substantial inter-annual variability, especially during 1980–2000 when extreme fire events were detected in 1982, 1987, 1991, 1994 and 1998. The occurrences of these extreme fires were associated with El Niño/Southern Oscillation (ENSO) events, especially in Indonesia (for example, the Great Fire of Borneo in 1982)[66]. Since 1997, N_2O emissions from fires estimated by DLEM, GFED4s and FAOSTAT were consistent in terms of inter-annual variability. All three estimates showed a decreasing trend, agreeing well with the satellite-observed decrease of the global burned area[64,65].

(c) Indirect emissions from anthropogenic nitrogen additions. Data were obtained from various sources and considered as nitrogen deposition on land and ocean ('Nitrogen deposition on land' and 'Nitrogen deposition on ocean'), as well as the nitrogen leaching and runoff from upstream ('Inland and coastal waters'). The emission from 'Nitrogen deposition on ocean' was provided in ref. [67], whereas emission from 'Nitrogen deposition on land' was the ensemble mean of an average of three inventories: FAOSTAT/EDGAR v4.3.2, GAINS/EDGAR v4.3.2 and NMIP. FAOSTAT and GAINS documented the sector 'Indirect agricultural N_2O emissions' by separating estimates from nitrogen leaching or nitrogen deposition, whereas EDGAR v4.3.2 did not. Here, we treated 'Indirect agricultural N_2O emissions' from EDGAR v4.3.2 as 'Inland and coastal waters' emissions for data synthesis. Only EDGAR v4.3.2 provided an estimate of indirect emission from non-agricultural sectors, whereas both FAOSTAT and GAINS—following the IPCC guidelines—provided NH_x/NO_y volatilization from agricultural sectors. Here, we sum FAOSTAT or GAINS data with EDGAR v4.3.2 data (that is, FAOSTAT/EDGAR v4.3.2 or GAINS/EDGAR v4.3.2) to represent nitrogen-deposition-induced soil emissions from both agricultural and non-agricultural sectors. The N_2O emissions from 'Inland and coastal waters' consist of emissions from rivers, reservoirs, lakes, estuaries and coastal zone, and is the ensemble mean of an average of three inventories (EDGAR v4.3.2, FAOSTAT, GAINS), and the mean of process-based models. The anthropogenic emission estimated in ref. [36] considered annual nitrogen inputs and other environmental factors (that is, climate, increased CO_2 and land cover change). For long-term average in rivers, reservoirs, estuaries and lakes, we applied a mean of 56% (based on the ratio of anthropogenic to total nitrogen additions from land) to calculate anthropogenic emissions. Seagrass, mangrove, saltmarsh and intertidal N_2O emissions were undated and obtained from ref. [68]. Coastal waters with low disturbance generally either have low N_2O emissions or act as a sink for N_2O[69,70]. Here, coastal zone emissions were treated as anthropogenic emissions owing to intensive human disturbances[71].

N_2O emissions after transport of anthropogenic nitrogen additions via the atmosphere and via water bodies increased from 1.1 (0.6–1.9) Tg N yr^{-1} in the 1980s to 1.3 (0.7–2.2) Tg N yr^{-1} during 2007–2016 (Table 1). The N_2O emissions from inland and coastal waters increased at a rate of 0.03 ± 0.00 Tg N yr^{-1} per decade (P < 0.05). Such an increase was reported by all three inventories (FAOSTAT, GAINS and EDGAR v4.3.2) with FAOSTAT giving the largest estimate. By contrast, the DLEM-based estimate presented a divergent trend: first increasing from 1980–1998 and then slightly decreasing thereafter (Extended Data Fig. 6a). Emissions from atmospheric nitrogen deposition on oceans were relatively constant with a value of 0.1 (0.1–0.2) Tg N yr^{-1}, whereas a large increase in emissions was found from atmospheric nitrogen deposition on land, with 0.06 ± 0.01 Tg N yr^{-1} per decade (P < 0.05) reported in the three estimates (FAOSTAT/EDGAR v4.3.2, GAINS/EDGAR v4.3.2 and NMIP). The FAOSTAT agricultural source—together with the EDGAR v4.3.2 industrial source—is consistent with NMIP estimates regarding the magnitude of N_2O emissions, with the latter estimating a slightly slower increase from 2010 to 2016 (Extended Data Fig. 6b).

(d) Perturbed fluxes from climate/CO_2/land cover change. Perturbed N_2O fluxes represent the sum of the effects of climate, increased atmospheric CO_2 and land cover change. The estimate of climate and CO_2 effects on emissions was based on NMIP. The effect of land cover change on N_2O dynamics includes the reduction due to 'Long-term effect of reduced mature forest area' and the emissions due to 'Post-deforestation pulse effect'. The two estimates were based on the book-keeping approach and the DLEM model simulation. The book-keeping method is developed in ref. [72] for accounting for carbon flows due to land use. In this study, an observation dataset consisting of 18 tropical sites was collected to follow the book-keeping logic. The dataset covers N_2O emissions from a reference mature forest and their nearby converted pastures aged between 1 and 60 years. The average tropical forest N_2O emission rate of 1.974 kg N_2O-N ha^{-1} yr^{-1} was adopted as the baseline[73]. Two logarithmic response curves of soil N_2O emissions (normalized to the baseline) after deforestation were developed: $y = -0.31\ln(x) + 1.53$ (R^2 = 0.30) and $y = -0.454\ln(x) + 2.21$ (R^2 = 0.09). The first logarithmic function uses data collected by a review analysis[74], and the second is based upon this but further considers observations from ref. [21] and ref. [75]. In the first function, x indicates pasture age in years after deforestation, and y (unitless; 0–1) indicates the ratio of pasture N_2O emission over the N_2O emission from the nearby reference mature forest. In the second function, x indicates secondary forest age and y indicates the ratio of secondary forest N_2O emission over that of a reference mature forest. This form of the response functions can effectively reproduce the short-lived increase in soil N_2O emissions after initial forest clearing and the gradually declining emission rates of converted crops and/or pastures[21,76]. Using these two curves and the baseline, we kept track of the N_2O reduction of tropical forests and the post-deforestation crop/pasture N_2O emissions at an annual timescale. This book-keeping method was applied to the two deforestation area datasets (Supplementary Information section 2.8), so we could investigate not only the difference caused by the two sets of land use data but also the difference between this empirical method and the process-based model. For land conversion from natural vegetation to croplands or pastures, DLEM uses a similar strategy to that used in ref. [72] and ref. [77] to simulate its influences on carbon and nitrogen cycles. Moreover, through using the sites of field observation from ref. [20] and ref. [75], we estimated N_2O emission from secondary tropical forests based on the algorithm: $y = 0.0084x + 0.2401$ (R^2 = 0.44). x indicates secondary forest age and y indicates the ratio of secondary forest N_2O emission over that of a reference mature forest. The difference between primary forests and secondary forests were subtracted from natural soil emissions simulated by six terrestrial biosphere models in NMIP.

We calculated the ensemble of oceanic N_2O emission based on the bottom-up approach (five ocean biogeochemical models; Supplementary Table 18) and the top-down approach (five estimates from four inversion models; Supplementary Table 19). The atmospheric burden and its rate of change during 1980–2016 were derived from mean maritime surface mixing ratios of N_2O (refs. [78,79]) with a conversion factor of 4.79 Tg N ppb^{-1} (ref. [80]). Combining uncertainties in measuring the mean surface mixing ratios[78] and that of converting surface mixing ratios to a global mean abundance[80], we estimate an uncertainty in the burden of ±1.4%. Annual change in atmospheric abundance is calculated from the combined NOAA and AGAGE record of surface N_2O and uncertainty is taken from the IPCC assessment report 5 (ref. [2]). There is an agreement between stratospheric loss from atmospheric chemistry transport models (top-down modelled chemical sink[18,81]) and satellite observations from a photolysis model (observed photochemical sink[1]), differing by only about 1 Tg N yr^{-1}. The satellite-based lifetime, 116 ± 9 yr, gives an overall uncertainty in the annual loss of ±8%. The tropospheric loss of N_2O from reaction with $O(^1D)$ is included in the observed atmospheric chemical sink (Table 1) and is small (around 1% of the stratospheric sink), with an estimated range of 0.1 to 0.2 Tg N yr^{-1}.

Comparison with the IPCC guidelines

The IPCC has provided guidance to quantify N_2O emissions, which is widely used in emission inventories for reporting to the UNFCCC. Over time the recommended approaches have changed, which is critical for estimating emissions from agricultural soils, the largest emission source. Previous global N_2O assessments[52,82,83] based on the IPCC 1996 guidelines[84] attributed about 6.3 Tg N yr^{-1} to the agricultural sector, including both direct and indirect emissions. This estimate is notably larger than our results (Fig. 1, Table 1) derived from multiple methods, and is also larger than the most recent estimates from global inventories (EDGAR v4.3.2, FAOSTAT and GAINS) that are based on the IPCC 2006 guidelines[14]. The main reason is that indirect emissions from leaching and groundwater were overestimated in previous studies[85]. Correspondingly, projections of atmospheric N_2O concentrations that are based on these overestimated emissions[82] led to biased estimates. For example, in ref. [82], atmospheric N_2O concentrations were expected to be 340–350 ppb in the year 2020, instead of 333 ppb[5] as observed. The 2019 Refinement to the 2006 IPCC Guidelines for National Greenhouse Gas Inventories has recently been published[86] and adopts the same approach for nitrogen application on soils, but considers the effects of different climate regimes. The new guidelines, which are based on a wealth of new scientific literature, proposed much smaller emissions from grazing animals, by a factor of 5–7. Our preliminary calculations indicate that global soil emissions based on these new guidelines may decrease by 20%–25%. Integrating estimates that rely on the IPCC methodology with estimates from process-based models provides for a more balanced assessment in this paper. We also added information from assessments[87,88] that derived agricultural emissions as the difference between atmospheric terms and other emissions such as combustion, industry and nature, and they gave comparable magnitudes (4.3–5.8 Tg N yr^{-1}) to our bottom-up results.

Uncertainty

Current data analysis and synthesis of long-term N_2O fluxes are based on a wide variety of top-down and bottom-up methods. Top-down approaches, consisting of four inversion frameworks[89–92], provide a wide range of estimates largely because of systematic errors in the modelled atmospheric transport and stratospheric loss of N_2O. In addition, the emissions from top-down analyses are dependent on the magnitude and distribution of the prior flux estimates to an extent that is strongly determined by the number of atmospheric N_2O measurements[18]. Inversions are generally not well constrained (and thus rely heavily on a priori estimates) in Africa, Southeast Asia, southern South America, and over the oceans, owing to the paucity of observations in these regions. The improvement of atmospheric transport models, more accurate priors, and more atmospheric N_2O measurements would reduce uncertainty in further top-down estimates, particularly for ocean and regional emissions.

Bottom-up approaches are subject to uncertainties in various sources from land[16] and oceans[32]. For process-based models (for example, NMIP and ocean biogeochemical models), the uncertainty is associated with differences in model configuration as well as process parameterization[16,32]. The uncertainty of estimates from NMIP could be reduced in several ways[16]. First, the six models in NMIP exhibited different spatial and temporal patterns of N_2O emissions even though they used the same forcings. Although these models have considered essential biogeochemical processes in soils (for example, biological nitrogen fixation, nitrification/denitrification, mineralization/immobilization, etc.)[93], some missing processes such as freeze–thaw cycles and ecosystem disturbances should be included in terrestrial biosphere models to reduce uncertainties. Second, the quality of input datasets—specifically the amount and timing of nitrogen application, and spatial and temporal changes in distribution of natural vegetation and agricultural land—is critical for accurately simulating soil N_2O emissions. Third, national and global N_2O flux measurement networks[17] could be used to validate model performance and to constrain large-scale model simulations. Data assimilation techniques could be used to improve model accuracy.

Current remaining uncertainty in global ocean model estimates of N_2O emission includes the contribution of N_2O flux derived from the tropical oceanic low oxygen zones (for example, the eastern Equatorial Pacific, the northern Indian ocean) relative to the global ocean. These low oxygen zones are predominantly influenced by high yield N_2O formation processes (for example, denitrification and enhanced nitrification). Regional observation-based assessments have also suggested that these regions may produce more N_2O than is simulated by the models[32]. The current generation of global ocean biogeochemistry models are not sufficiently accurate to represent the high N_2O production processes in low-oxygen zones and their associated variability (see refs. [34,94,95] for more detail). Thus, precisely representing the local ocean circulation and associated biogeochemical fluxes of these regions could further reduce the uncertainty in estimates of global and regional oceanic N_2O emissions.

Regardless of the tier approach used, greenhouse-gas inventories for agriculture suffer from high uncertainty in the underlying agriculture and rural data and statistics used as input, including statistics on fertilizer use, livestock manure availability, storage and applications, and nutrient, crop and soils management. For instance, animal waste management is an uncertain aspect, because much of the manure is either not used, or is used as a fuel or building material, or may be discharged directly to surface water[96], with important repercussions for the calculated emissions. Furthermore, greenhouse-gas inventories using default emission factors show large uncertainties at local to global scales, especially for agricultural N_2O emissions, due to the poorly captured dependence of emission factors on spatial diversity in climate, management, and soil physical and biochemical conditions[2,22]. It is well known, for example from the IPCC guidelines, that higher-tier greenhouse-gas inventories may provide more reasonable estimates by using the alternative emission factors that are disaggregated by environmental factors and management-related factors[86]. A large range of emission factors have been used to estimate aquaculture N_2O emissions[31,39,62,87], and long-term estimates of nitrogen flows in freshwater and marine aquaculture are scarce[30]. Uncertainty also remains in several N_2O sources that have not yet been fully understood or quantified. To date, robust estimates of N_2O emissions from global peatland degradation are still lacking, although we have accounted for N_2O emissions due to the drainage of organic soils (histosols) obtained from FAOSTAT and GAINS databases[28,41]. Recent evidence shows that permafrost thawing[97] and the freeze–thaw cycle[98] contribute to increasing N_2O emissions; however, are not well established in the current estimates of the global N_2O budget.

Statistics

The Mann–Kendall test in R-3.4.4 was used to assess the significance of trends in annual N_2O emissions from each sub-sector based on the bottom-up approach.

Data availability

The relevant datasets of this study are archived in the box site of the International Center for Climate and Global Change Research at Auburn University (https://auburn.box.com/). Researchers that are interested in using the results made available in the repository are encouraged to contact the original data providers.

Code availability

The relevant codes used in this study are archived in the box site of the International Center for Climate and Global Change Research at Auburn University (https://auburn.box.com/).

50. Nevison, C. D., Lueker, T. J. & Weiss, R. F. Quantifying the nitrous oxide source from coastal upwelling. *Glob. Biogeochem. Cycles* **18**, GB1018 (2004).
51. Lauerwald, R. et al. Natural lakes are a minor global source of N_2O to the atmosphere. *Glob. Biogeochem. Cycles* **33**, 1564–1581 (2019).
52. Kroeze, C., Mosier, A. & Bouwman, L. Closing the global N_2O budget: a retrospective analysis 1500–1994. *Glob. Biogeochem. Cycles* **13**, 1–8 (1999).
53. Schumann, U. & Huntrieser, H. The global lightning-induced nitrogen oxides source. *Atmos. Chem. Phys.* **7**, 3823–3907 (2007).
54. De Klein, C. et al. N_2O emissions from managed soils, and CO_2 emissions from lime and urea application. In *2006 IPCC Guidelines for National Greenhouse Gas Inventories* Vol. 4, Ch. 11 (IPCC, 2006).
55. Dentener, F. J. & Crutzen, P. J. A three-dimensional model of the global ammonia cycle. *J. Atmos. Chem.* **19**, 331–369 (1994).
56. Röckmann, T., Kaiser, J., Crowley, J. N., Brenninkmeijer, C. A. & Crutzen, P. J. The origin of the anomalous or "mass-independent" oxygen isotope fractionation in tropospheric N_2O. *Geophys. Res. Lett.* **28**, 503–506 (2001).
57. Kaiser, J. & Röckmann, T. Absence of isotope exchange in the reaction of N_2O+$O(^1D)$ and the global $\Delta^{17}O$ budget of nitrous oxide. *Geophys. Res. Lett.* **32**, L15808 (2005).
58. Schlesinger, W. H. An estimate of the global sink for nitrous oxide in soils. *Glob. Change Biol.* **19**, 2929–2931 (2013).
59. Syakila, A., Kroeze, C. & Slomp, C. P. Neglecting sinks for N_2O at the Earth's surface: does it matter? *J. Integr. Environ. Sci.* **7**, 79–87 (2010).
60. Bouwman, A. F. et al. Hindcasts and future projections of global inland and coastal nitrogen and phosphorus loads due to finfish aquaculture. *Rev. Fish. Sci.* **21**, 112–156 (2013).
61. Bouwman, A. F. et al. Global hindcasts and future projections of coastal nitrogen and phosphorus loads due to shellfish and seaweed aquaculture. *Rev. Fish. Sci.* **19**, 331–357 (2011).
62. Hu, Z., Lee, J. W., Chandran, K., Kim, S. & Khanal, S. K. Nitrous oxide (N_2O) emission from aquaculture: a review. *Environ. Sci. Technol.* **46**, 6470–6480 (2012).
63. Williams, J. & Crutzen, P. J. Nitrous oxide from aquaculture. *Nat. Geosci.* **3**, 143 (2010).
64. Andela, N. et al. A human-driven decline in global burned area. *Science* **356**, 1356–1362 (2017).
65. Yang, J. et al. Spatial and temporal patterns of global burned area in response to anthropogenic and environmental factors: reconstructing global fire history for the 20th and early 21st centuries. *J. Geophys. Res. Biogeosci.* **119**, 249–263 (2014).
66. Dennis, R. *A Review of Fire Projects in Indonesia (1982–1998)* (Center for International Forestry Research, 1999).
67. Suntharalingam, P. et al. Quantifying the impact of anthropogenic nitrogen deposition on oceanic nitrous oxide. *Geophys. Res. Lett.* **39**, L07605 (2012).
68. Murray, R. H., Erler, D. V. & Eyre, B. D. Nitrous oxide fluxes in estuarine environments: response to global change. *Glob. Change Biol.* **21**, 3219–3245 (2015).
69. Erler, D. V. et al. Applying cavity ring-down spectroscopy for the measurement of dissolved nitrous oxide concentrations and bulk nitrogen isotopic composition in aquatic systems: correcting for interferences and field application. *Limnol. Oceanogr. Methods* **13**, 391–401 (2015).
70. Murray, R., Erler, D., Rosentreter, J. & Eyre, B. Seasonal and spatial N_2O concentrations and emissions in three tropical estuaries. *Mar. Chem.* **221**, 103779 (2020).
71. Vernberg, F. J. & Vernberg, W. B. *The Coastal Zone: Past, Present, and Future* (Univ. South Carolina Press, 2001).
72. Houghton, R. et al. Changes in the carbon content of terrestrial biota and soils between 1860 and 1980: a net release of CO_2 to the atmosphere. *Ecol. Monogr.* **53**, 235–262 (1983).
73. Davidson, E. A. The contribution of manure and fertilizer nitrogen to atmospheric nitrous oxide since 1860. *Nat. Geosci.* **2**, 659–662 (2009).
74. van Lent, J., Hergoualc'h, K. & Verchot, L. V. Soil N_2O and NO emissions from land use and land-use change in the tropics and subtropics: a meta-analysis. *Biogeosciences* **12**, 7299–7313 (2015).
75. Keller, M. & Reiners, W. A. Soil–atmosphere exchange of nitrous oxide, nitric oxide, and methane under secondary succession of pasture to forest in the Atlantic lowlands of Costa Rica. *Glob. Biogeochem. Cycles* **8**, 399–409 (1994).
76. Melillo, J. M. et al. Nitrous oxide emissions from forests and pastures of various ages in the Brazilian Amazon. *J. Geophys. Res. D* **106**, 34179–34188 (2001).
77. McGuire, A. et al. Carbon balance of the terrestrial biosphere in the twentieth century: Analyses of CO_2, climate and land use effects with four process-based ecosystem models. *Glob. Biogeochem. Cycles* **15**, 183–206 (2001).
78. Dlugokencky, E., Steele, L., Lang, P. & Masarie, K. The growth rate and distribution of atmospheric methane. *J. Geophys. Res. D* **99**, 17021–17043 (1994).
79. IPCC 2013. Annex II: Climate System Scenario Tables (eds Prather, M. et al.). In *Climate Change 2013: The Physical Science Basis* (eds Stocker, T. F. et al.) (Cambridge Univ. Press, 2013).
80. Prather, M. J., Holmes, C. D. & Hsu, J. Reactive greenhouse gas scenarios: systematic exploration of uncertainties and the role of atmospheric chemistry. *Geophys. Res. Lett.* **39**, L09803 (2012).
81. Prather, M. J. & Hsu, J. Coupling of nitrous oxide and methane by global atmospheric chemistry. *Science* **330**, 952–954 (2010).
82. Mosier, A. & Kroeze, C. Potential impact on the global atmospheric N_2O budget of the increased nitrogen input required to meet future global food demands. *Chemosphere* **2**, 465–473 (2000).
83. Mosier, A. et al. Closing the global N_2O budget: nitrous oxide emissions through the agricultural nitrogen cycle. *Nutr. Cycl. Agroecosyst.* **52**, 225–248 (1998).
84. Houghton, J. T. et al (eds) *Revised 1996 IPCC Guidelines for National Greenhouse Gas Inventories* Vols 1–3 (IPCC, 1997).
85. Nevison, C. Indirect N_2O emissions from agriculture. In *Background Papers: IPCC Expert Meetings on Good Practice Guidance and Uncertainty Management in National Greenhouse Gas Inventories* 381–397 (IPCC, 2000).
86. *2019 Refinement to the 2006 IPCC Guidelines for National Greenhouse Gas Inventories* Vol. 4 (IPCC, 2019).
87. Crutzen, P. J., Mosier, A. R., Smith, K. A. & Winiwarter, W. N_2O release from agro-biofuel production negates global warming reduction by replacing fossil fuels. *Atmos. Chem. Phys.* **8**, 389–395 (2008).
88. Smith, K. A., Mosier, A. R., Crutzen, P. J. & Winiwarter, W. The role of N_2O derived from crop-based biofuels, and from agriculture in general, in Earth's climate. *Phil. Trans. R. Soc. Lond. B* **367**, 1169–1174 (2012).
89. Thompson, R. L. et al. Nitrous oxide emissions 1999 to 2009 from a global atmospheric inversion. *Atmos. Chem. Phys.* **14**, 1801–1817 (2014).
90. Wells, K. C. et al. Simulation of atmospheric N_2O with GEOS-Chem and its adjoint: evaluation of observational constraints. *Geosci. Model Dev.* **8**, 3179–3198 (2015).
91. Wilson, C., Chipperfield, M., Gloor, M. & Chevallier, F. Development of a variational flux inversion system (INVICAT v1. 0) using the TOMCAT chemical transport model. *Geosci. Model Dev.* **7**, 2485–2500 (2014).
92. Patra, P. K. et al. Improved chemical tracer simulation by MIROC4.0-based atmospheric chemistry-transport model (MIROC4-ACTM). *SOLA* **14**, 91–96 (2018).
93. Tian, H. Q. et al. The global N_2O Model Intercomparison Project. *Bull. Am. Meteorol. Soc.* **99**, 1231–1251 (2018).
94. Suntharalingam, P. et al. Anthropogenic nitrogen inputs and impacts on oceanic N_2O fluxes in the northern Indian Ocean: the need for an integrated observation and modelling approach. *Deep Sea Res. Part II* **166**, 104–113 (2019).
95. Battaglia, G. & Joos, F. Marine N_2O emissions from nitrification and denitrification constrained by modern observations and projected in multimillennial global warming simulations. *Glob. Biogeochem. Cycles* **32**, 92–121 (2018).
96. Galloway, J. et al. The impact of animal production systems on the nitrogen cycle. In *Livestock in a Changing Landscape* Vol. 1 (eds Steinfeld, H. et al.) 83–95 (Island Press, 2010).
97. Elberling, B., Christiansen, H. H. & Hansen, B. U. High nitrous oxide production from thawing permafrost. *Nat. Geosci.* **3**, 332–335 (2010).
98. Wagner-Riddle, C. et al. Globally important nitrous oxide emissions from croplands induced by freeze–thaw cycles. *Nat. Geosci.* **10**, 279–283 (2017).
99. Suntharalingam, P. et al. Estimates of oceanic nitrous-oxide emissions from global biogeochemistry models. In *American Geophysical Union, Fall Meeting 2018* B21K-2481B (2018).
100. Janssens-Maenhout, G. et al. EDGAR v4.3.2 Global Atlas of the three major greenhouse gas emissions for the period 1970–2012. *Earth Syst. Sci. Data* **11**, 959–1002 (2019).
101. Tubiello, F. et al. *Estimating Greenhouse Gas Emissions in Agriculture* Ch. 5, 35–115 (FAO, 2015).
102. van der Werf, G. R. et al. Global fire emissions estimates during 1997–2016. *Earth Syst. Sci. Data* **9**, 697–720 (2017).
103. Dentener, F. Global maps of atmospheric nitrogen deposition, 1860, 1993, and 2050. https://doi.org/10.3334/ORNLDAAC/830 (Oak Ridge National Laboratory, 2006).
104. Riahi, K. et al. The Shared Socioeconomic Pathways and their energy, land use, and greenhouse gas emissions implications: an overview. *Glob. Environ. Change* **42**, 153–168 (2017).

Acknowledgements This paper is the result of a collaborative international effort under the umbrella of the Global Carbon Project (a project of Future Earth and a research partner of the World Climate Research Programme) and International Nitrogen Initiative. This research was made possible partly by Andrew Carnegie Fellowship award no. G-F-19-56910; NSF grant nos 1903722,1243232 and 1922687; NASA grant nos NNX14AO73G, NNX10AU06G, NNX11AD47G and NNX14AF93G; NOAA grant nos NA16NOS4780207 and NA16NOS4780204; National Key R&D Program of China (grant no. 2017YFA0604702); National Natural Science Foundation of China (grant no. 41961124006); and OUC-AU Joint Center Program. E.T.B., P.R., G.P.P., R.L.T. and P.S. acknowledge funding support from VERIFY project (EC H2020 grant no. 776810); P.S. also acknowledges funding from the EC H2020 grant no. 641816 (CRESCENDO); A.I. acknowledges funding support from JSPS KAKENHI grant (no. 17H01867); G.B., F.J. and S.L. acknowledge support from the Swiss National Science Foundation (no. 200020_172476) and EC H2020 grant no. 821003 (Project 4C) and no. 820989 (Project COMFORT); A.L. acknowledges support from DFG project SFB754/3; S.Z. acknowledges support from EC H2020 grant no. 647204; K.C.W. and D.B.M. acknowledge support from NASA (IDS grant no. NNX17AK18G) and NOAA (grant no. NA13OAR4310086); P.A.R. acknowledges NASA Award NNX17AI74G; M.M. acknowledges support from the Scottish Government's Rural and Environment Science and Analytical Services Division (RESAS) Environmental Change Programme (2016-2021); B.D.E. acknowledges the support from ARC Linkage Grants LP150100519 and LP190100271; M.J.P. acknowledges the US Department of Energy grant no. DE-SC0012536, Lawrence Livermore National Laboratory B628407 and NASA MAP program grant no. NNX13AL12G; S.B. was supported by the EC H2020 with the CRESCENDO project (grant no. 641816) and by the COMFORT project (grant no. 820989), and also acknowledges the support of the team in charge of the CNRM-CM climate model; F.Z. acknowledges the support from the National Natural Science Foundation of China (41671464). Supercomputing time was provided by the Météo-France/DSI supercomputing center. P.K.P. is partly supported by Environment Research and Technology Development Fund (#2-1802) of the Ministry of the Environment, Japan; R.L. acknowledges support from the French state aid managed by the ANR under the 'Investissements d'avenir' programme with the reference ANR-16-CONV-0003. NOAA ground-based observations of atmospheric N_2O are supported by NOAA's Climate Program Office under the Atmospheric Chemistry Carbon Cycle and Climate (AC4) theme. The AGAGE stations measuring N_2O are supported by NASA (USA) grants NNX16AC98G to MIT and NNX16AC97G and NNX16AC96G to SIO, and by BEIS (UK) for Mace Head, NOAA (USA) for Barbados, and CSIRO and BoM (Australia) for Cape Grim. F.N.T. acknowledges funding from FAO regular programme. The views expressed in this publication are those of the author(s) and do not necessarily reflect the views or policies of FAO. P.C. acknowledges support from ERC Synergy Grant Imbalance-P and the ANR Cland Convergence Institute. We also thank S. Frolking for constructive comments and suggestions that have helped to improve this paper. The statements made and views expressed are solely the responsibility of the authors.

Author contributions H.T., R.L.T., J.G.C. and R.B.J. designed and coordinated the study. H.T., R.X., J.G.C., R.L.T., W.W., P.S., E.A.D., P.C., R.B.J., G.J.-M., M.J.P., N.P., S.P., P.R., H.S., F.N.T., S.Z., F.Z., B.F. and G.P.P. conducted data analysis, synthesis and wrote the paper. R.L.T. led atmospheric inversions teaming with M.P.C., D.B.M., P.K.P., K.C.W. and C.W.; H.T. led land biosphere modelling teaming with P.C., H.S., S.Z., A.A., F.J., J.C., S.R.S.D., A.I., W.L., S.L., S.O., N.V., E.A.D. and S.D.; P.S. led ocean biogeochemical modelling teaming with G.B., L.B., S.B., E.T.B., F.J. and A.L.; P.R. led inland water and coastal modelling and synthesis teaming with B.D.E., G.G.L., R.L., T.M., P.A.R., H.T. and Y.Y.; A.F.B., J.W. and M.M. provided data of N_2O flux in aquaculture. G.R.v.d.W. and J.Y. provided data of N_2O emissions from biomass burning. F.Z. provided cropland N_2O flux data from a statistical model and field observations. G.J.M., F.N.T. and W.W. provided N_2O inventory data. M.J.P. and D.J.R. provided data of stratospheric and tropospheric sinks. G.P.P. provided RCP and SSP scenarios data and analysis. B.H., E.D. and J.W.E. provided a global N_2O monitoring dataset from NOAA/ESRL GMD. R.G.P. and R.F.W. provided a global N_2O monitoring dataset from AGAGE stations. P.B.K. provided a global N_2O monitoring dataset from CSIRO. All co-authors reviewed and commented on the manuscript.

Competing interests The authors declare no competing interests.

Additional information

Supplementary information is available for this paper at https://doi.org/10.1038/s41586-020-2780-0.

Correspondence and requests for materials should be addressed to H.T.

Peer review information *Nature* thanks Steve Frolking, Arvin Mosier and the other, anonymous, reviewer(s) for their contribution to the peer review of this work.

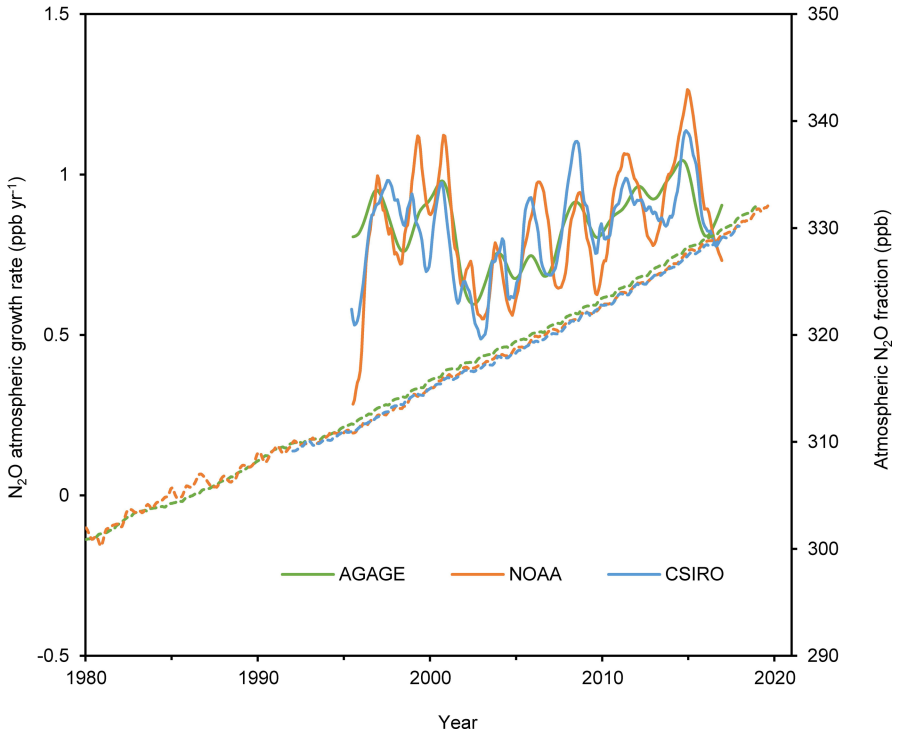

Extended Data Fig. 1 | Global mean growth rates and atmospheric concentration of N_2O. Global mean growth rates (solid lines, during 1995–2017) and atmospheric N_2O concentration (dashed lines, during 1980–2017) are from the AGAGE[6] (green), NOAA[5] (orange) and CSIRO (blue) networks. Global mean growth rates were calculated with annual time steps and are shown as 12-month moving averages. Growth rates are not calculated before 1995 owing to insufficient data and higher uncertainties on the measurements.

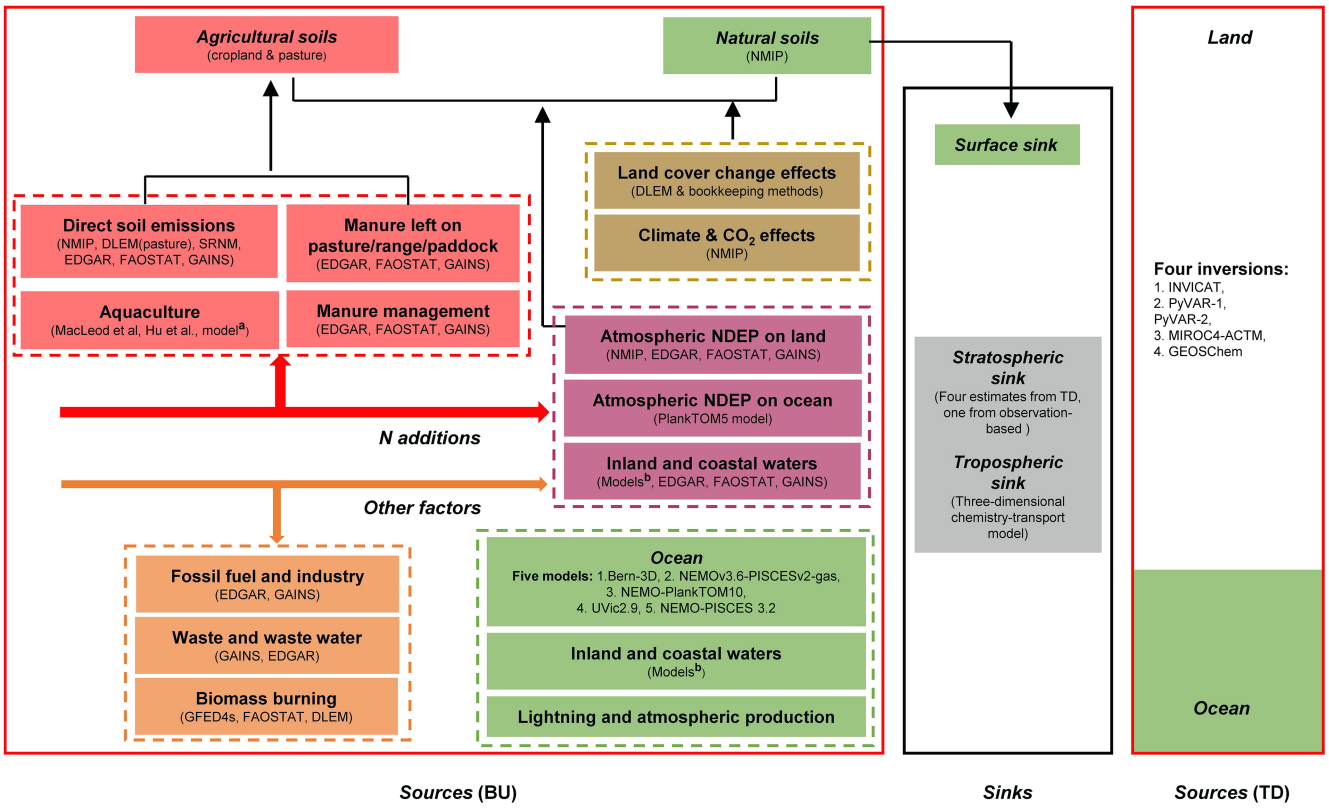

Extended Data Fig. 2 | The methodology for data synthesis of the global N_2O budget. BU and TD represent bottom-up and top-down methods, respectively. The colour codes are the same as that used in Table 1 and Figs. 1–3. We use both approaches, including 22 bottom-up and five top-down estimates of N_2O fluxes from land and oceans. For sources estimated by the bottom-up approach, we include six process-based terrestrial biosphere modelling studies[16]; five process-based ocean biogeochemical models[99]; one nutrient budget model[30,60,61]; five inland water modelling studies[35,36,50,51,68]; one statistical model SRNM based on spatial extrapolation of field measurements[17]; and four greenhouse-gas inventories: EDGAR v4.3.2[100], FAOSTAT[101], GAINS[41], and GFED4s[102]. In addition, previous studies regarding estimates of surface sink[58,73], lightning[53,54], atmospheric production[56,57,103], aquaculture[31,62] and model-based tropospheric sink[81] and observed stratospheric sink[1] are included in the current synthesis. [a]Ref. [31] and ref. [62] provide global aquaculture N_2O emissions in 2013 and in 2009, respectively; and the nutrient budget model[30,60,61] provides nitrogen flows in global freshwater and marine aquaculture over the period 1980–2016. [b]Model-based estimates of N_2O emissions from inland and coastal waters include rivers and reservoirs[35,36], lakes[51], estuaries[35], coastal zones (that is, seagrasses, mangroves, saltmarsh and intertidal saltmarsh)[68] and coastal upwelling[50].

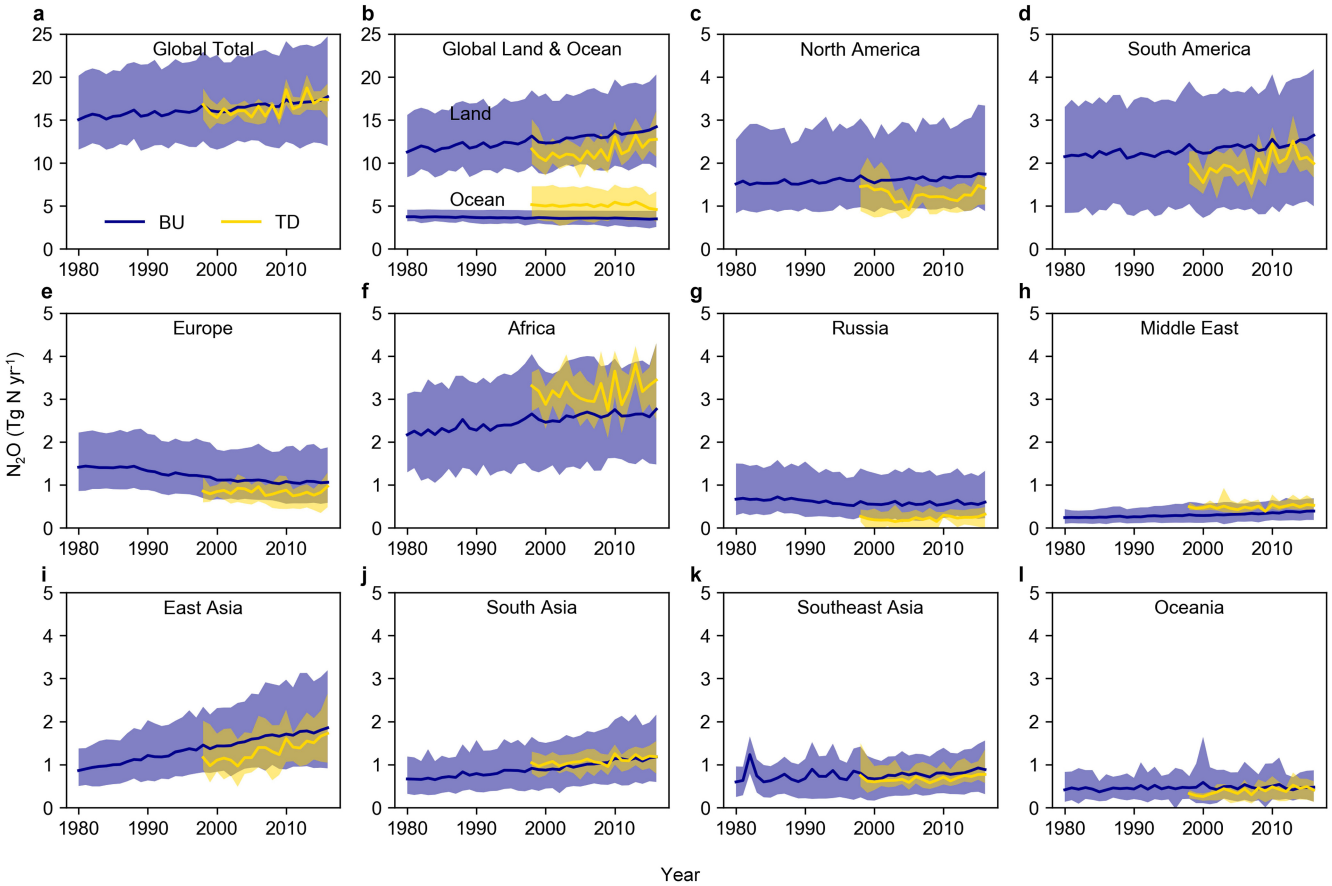

Extended Data Fig. 3 | Comparison of annual total N_2O emissions at global and regional scales estimated by bottom-up and top-down approaches. The blue lines represent the mean N_2O emission from bottom-up methods and the shaded areas show minimum and maximum estimates; the gold lines represent the mean N_2O emission from top-down methods and the shaded areas show minimum and maximum estimates.

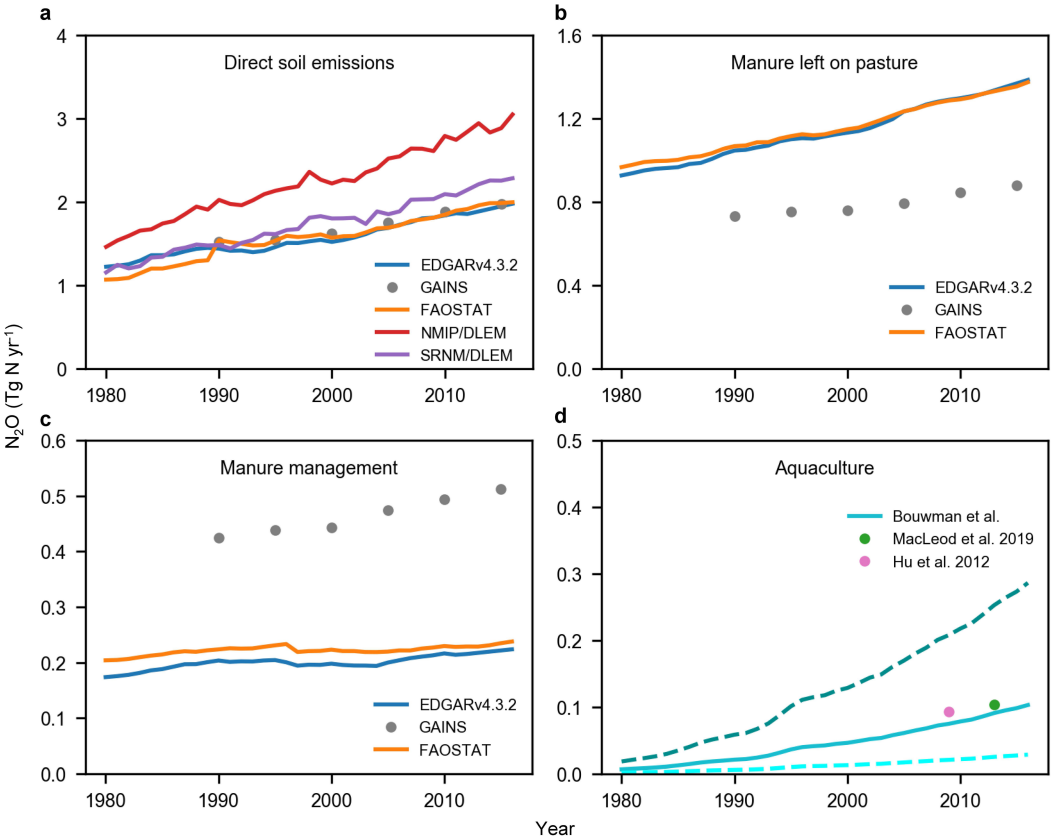

Extended Data Fig. 4 | Global agricultural N_2O emissions. a, Direct emission from agricultural soils associated with mineral fertilizer, manure and crop residue inputs, and cultivation of organic soils based on EDGAR v4.3.2, GAINS, FAOSTAT, NMIP/DLEM and SRNM/DLEM estimates. NMIP/DLEM or SRNM/DLEM indicates the combination of N_2O emission estimated by NMIP or SRNM from croplands with N_2O emission from intensively managed grassland (pasture) by estimated by DLEM. **b**, Direct emission from the global total area under permanent meadows and pasture, due to manure nitrogen deposition (left on pasture) based on EDGAR v4.3.2, FAOSTAT and GAINS estimates. **c**, Emission from manure management based on FAOSTAT, GAINS and EDGAR v4.3.2. **d**, Aquaculture N_2O emission based on a nutrient budget model[30], ref. [31] and ref. [62]; the solid line represents the 'best estimate' that is the product of emission factor (1.8%) and nitrogen waste from aquaculture provided by the nutrient budget model; the dashed lines represent the minimum and maximum values.

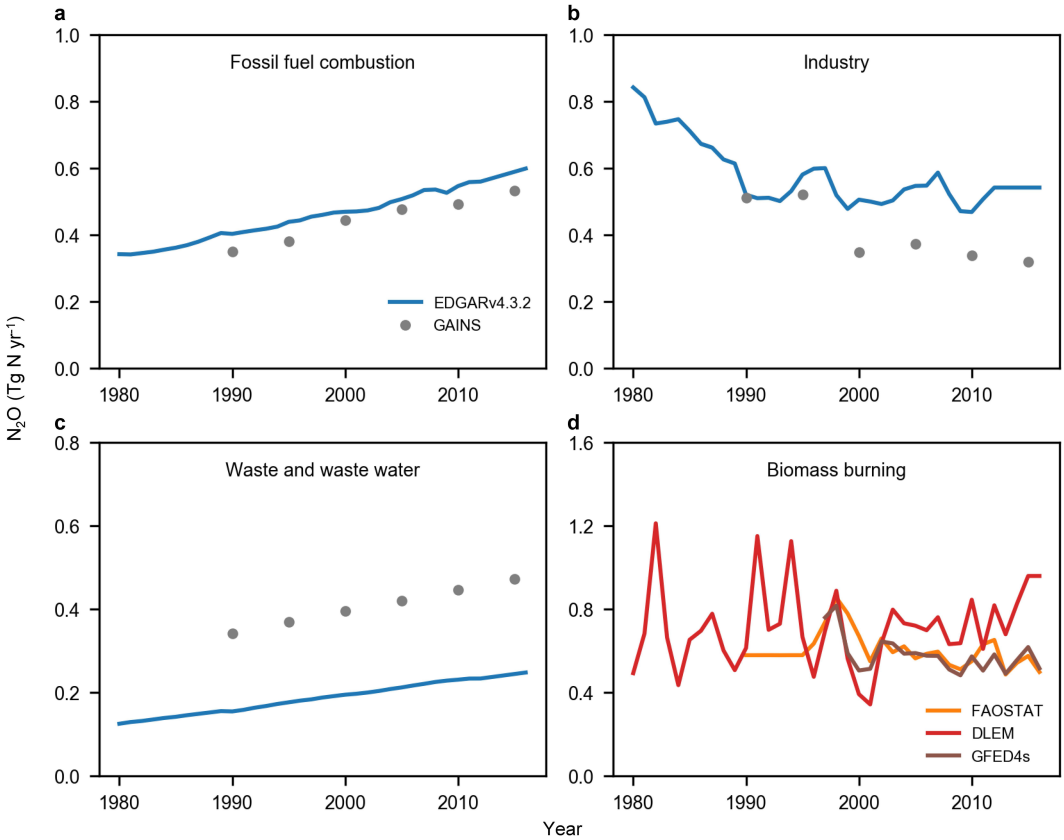

Extended Data Fig. 5 | Global N_2O emission from other direct anthropogenic sources. a, Emission from fossil fuel combustion based on EDGAR v4.3.2 and GAINS estimates. **b**, Emission from industry based on EDGAR v4.3.2 and GAINS estimates. **c**, Emission from waste and waste water based on EDGAR v4.3.2 and GAINS estimates. **d**, Emission from biomass burning based on FAOSTAT, DLEM, and GFED4s estimates.

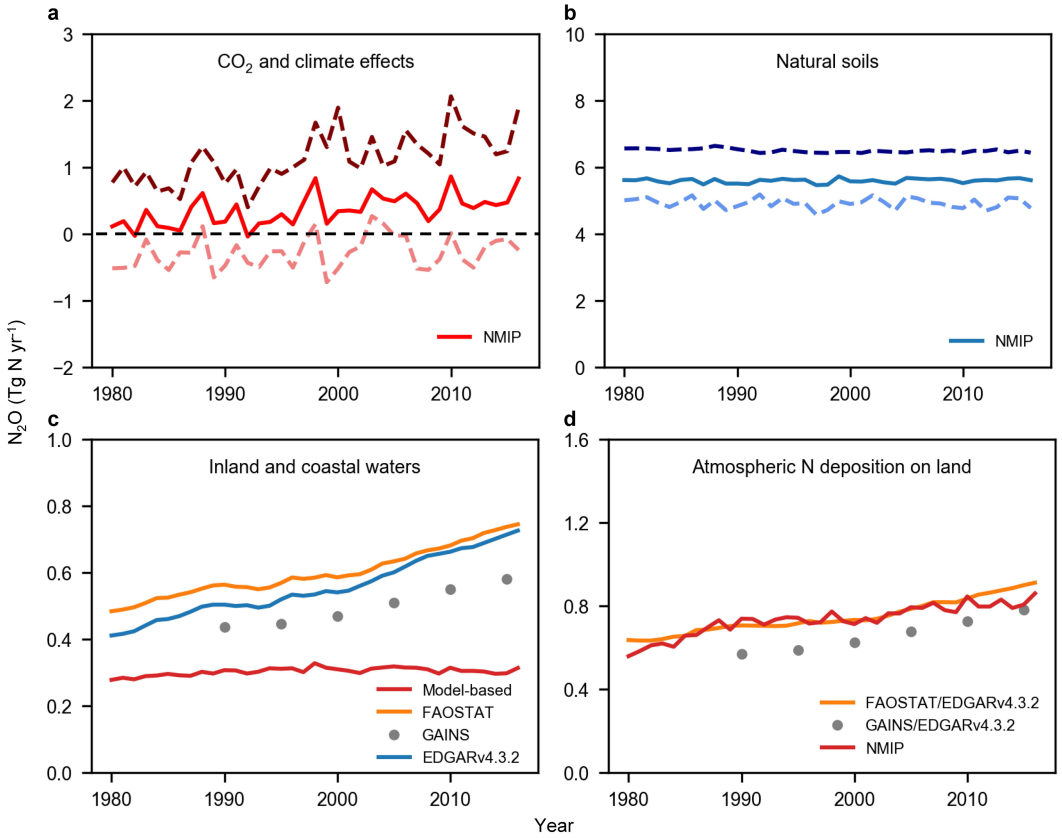

Extended Data Fig. 6 | Global N_2O emissions from natural soils, inland and coastal waters and due to change in climate, atmospheric CO_2 and nitrogen deposition. **a**, Changes in global soil N_2O fluxes due to changing CO_2 and climate. **b**, Global natural soil N_2O emissions without consideration of land use change (for example, deforestation) and without consideration of indirect anthropogenic effects via global change (that is, climate, increased CO_2 and atmospheric nitrogen deposition). The estimates are based on NMIP estimates during 1980–2016 including six process-based land biosphere models. Here, we also subtracted the difference between including and not including emissions from secondary forests (that grow back after pasture or cropland abandonment) as part of natural soil emissions based on NMIP estimates. The solid lines represent the ensemble and dashed lines show the minimum and maximum values. **c**, Global anthropogenic N_2O emission from inland waters, estuaries, coastal zones based on models (model-based), FAOSTAT, GAINS and EDGAR v4.3.2 estimates. **d**, Emission due to atmospheric nitrogen deposition on land based on NMIP, FAOSTAT/EDGAR v4.3.2 and GAINS/EDGAR v4.3.2. FAOSTAT/EDGAR v4.3.2 or GAINS/EDGAR v4.3.2 indicates the combination of agricultural source estimates from FAOSTAT or GAINS with non-agricultural source estimates from EDGAR v4.3.2. A process-based model DLEM[36] and a mechanistic stochastic model[35,51] were used to estimate N_2O emission from inland waters and estuaries, whereas site-level emission rates of N_2O were upscaled to estimate global N_2O fluxes from the global seagrass area[68].

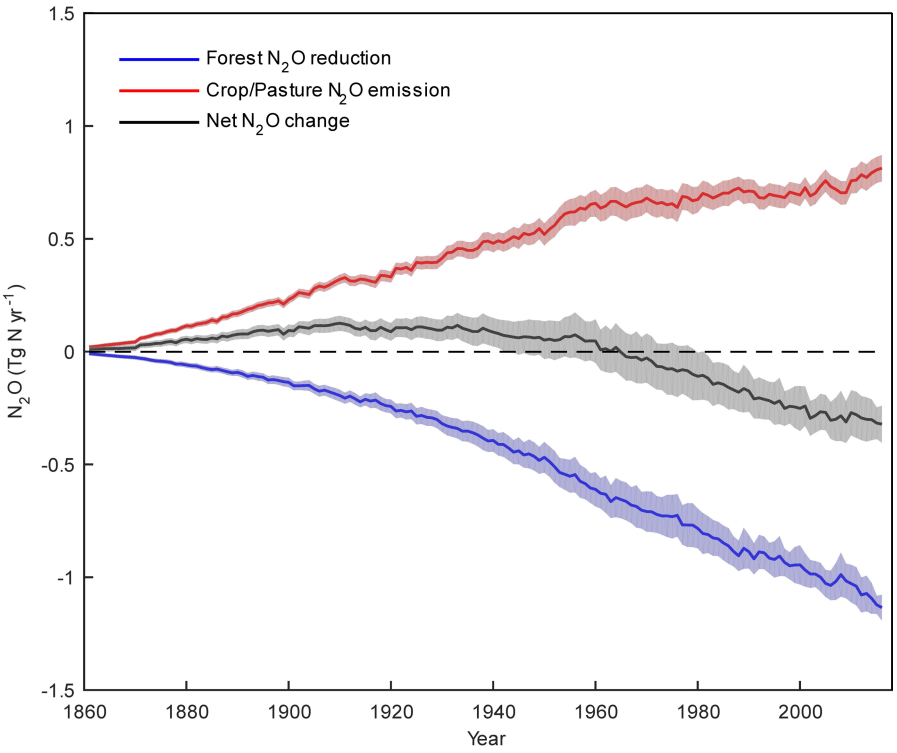

Extended Data Fig. 7 | Global N_2O dynamics due to land cover changes. The blue line represents the mean forest N_2O reduction caused by the long-term effect of reduced mature forest area (that is, deforestation) and shaded areas show minimum and maximum estimates; the red line represents the mean N_2O emission from the post-deforestation pulse effect (that is, crop/pasture N_2O emissions from legacy nitrogen of previous forest soil, not accounting for new fertilizer nitrogen added to these crop/pasture lands) and shaded areas show minimum and maximum estimates; the grey line represents the mean net deforestation emission of N_2O and shaded areas show minimum and maximum estimates.

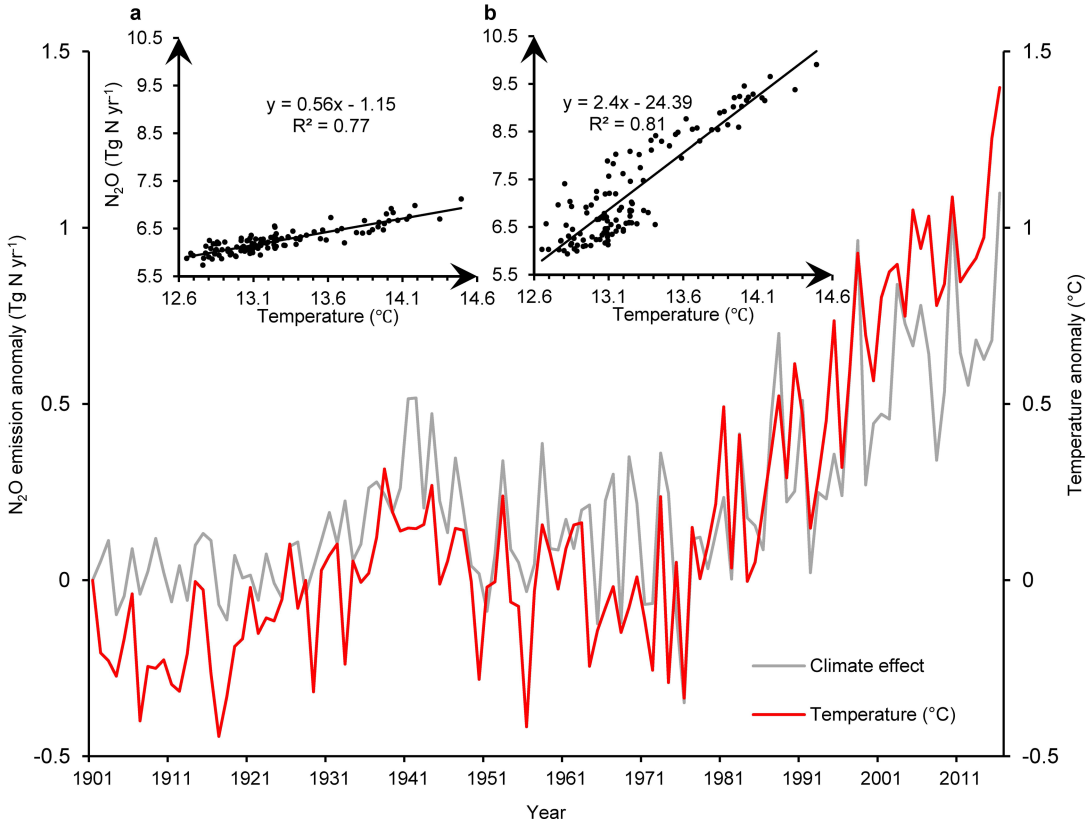

Extended Data Fig. 8 | Global simulated N_2O emission anomaly due to climate effect and global annual land surface temperature anomaly during 1901–2016. Global N_2O emission anomalies are the ensemble of six process-based land biosphere models in NMIP. The temperature data were obtained from the CRU-NCEP v8 climate dataset (https://vesg.ipsl.upmc.fr). **a**, The correlation between average global annual land surface temperature and simulated N_2O emissions (that is, the result of SE6 experiment in NMIP[16]) considering annual changes in climate but keeping all other factors (that is, nitrogen fertilizer, manure, NDEP, increased CO_2 and land cover change) at the level of 1860. **b**, The correlation between average global annual land surface temperature and simulated N_2O emissions (that is, the result of SE1 experiment in NMIP[16]) considering annual changes in all factors during 1860–2016.

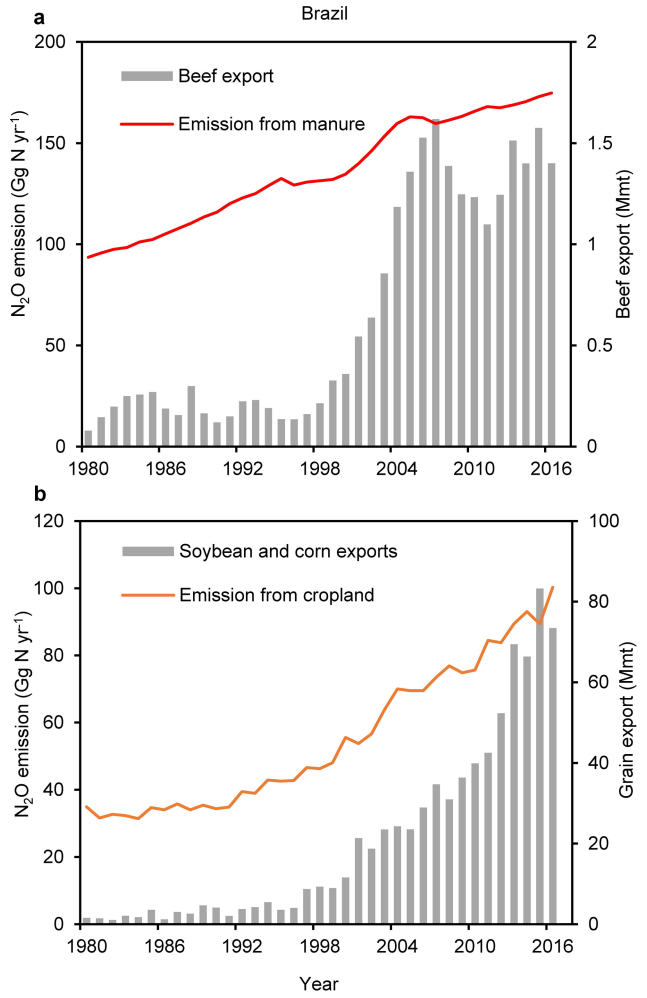

Extended Data Fig. 9 | Direct soil emissions and agricultural product trades in Brazil. a, The red line shows the ensemble direct N_2O emissions from livestock manure based on EDGAR v4.3.2, GAINS and FAOSTAT, the sum of 'manure left on pasture' and 'manure management'. The grey columns show the amount of beef exported by Brazil. **b**, Orange line shows the ensemble direct N_2O emissions from croplands due to nitrogen fertilization based on NMIP and SRNM. The grey columns show the amount of soybeans and corn exported by Brazil. Data regarding beef and cereal product exports were adapted from the ABIEC (beef) and FAOSTAT (soybean and corn) databases. Mmt yr^{-1} represents millions of metric tons per year.

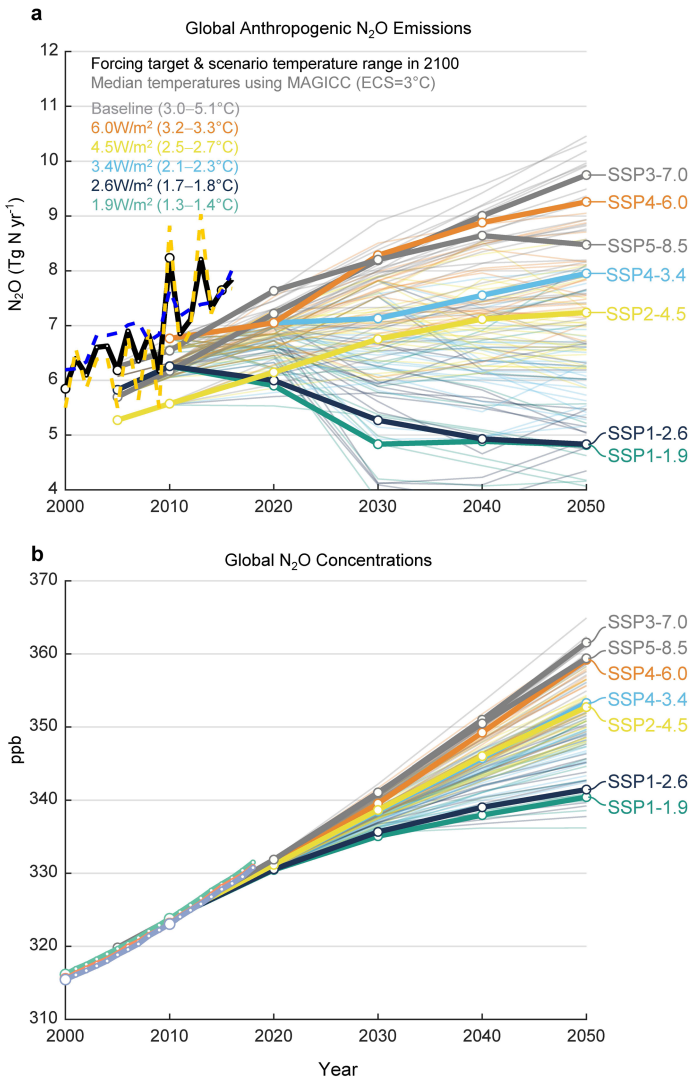

Extended Data Fig. 10 | A comparison of anthropogenic N_2O emissions and atmospheric N_2O concentrations in the unharmonized SSPs. An extension of Fig. 4, in which the emission and concentration data are the same as in Fig. 4. **a**, Global anthropogenic N_2O emissions; **b**, Global N_2O concentrations. The unharmonized emissions from the Integrated Assessment Models (IAMs)[104] show a large variation due to different input data and model assumptions. Comparison with Fig. 4b, d illustrates the modifications to the IAM scenario data for use in CMIP6. All baseline scenarios (SSP 3–7.0 and SSP 5–8.5; without climate policy applied) are shown in grey regardless of the radiative forcing level they reach in 2100.